Water Resources Research

RESEARCH ARTICLE
10.1029/2024WR038410

Seasonality Controls Biogeochemical Shifts in Oxygen, Carbon, and Nitrogen Along a 12-m, 54 hr-Long Hyporheic Flowpath

S. P. Herzog[1], A. S. Ward[2], S. M. Wondzell[3], S. P. Serchan[4], R. González-Pinzón[5], and J. P. Zarnetske[6]

[1]Natural Resources Program, Department of Forest Ecosystems & Society, College of Forestry, Oregon State University-Cascades, Bend, OR, USA, [2]Biological and Ecological Engineering Department, Oregon State University, Corvallis, OR, USA, [3]Pacific Northwest Research Station, Forest Service, United States Department of Agriculture, Corvallis, OR, USA, [4]Department of Geology and Geosciences, University of Vermont, Burlington, VT, USA, [5]Gerald May Department of Civil, Construction & Environmental Engineering, University of New Mexico, Albuquerque, NM, USA, [6]Department of Earth and Environmental Science, Michigan State University, East Lansing, MI, USA

Key Points:

- Seasonal fluctuations in the oxic-anoxic boundary of at least 6-m shifted net nitrogen source/sink behavior and rates of carbon cycling
- Prevalent in situ C and N were more important than influent chemistry, sustaining most reactions at zeroth-order rates for 12-m and 54-hr
- Decameter-scale hyporheic flowpaths can be reaction- and transport-limited for different solutes, potentially impacting water quality

Supporting Information:

Supporting Information may be found in the online version of this article.

Correspondence to:

S. P. Herzog,
herzogs@oregonstate.edu

Citation:

Herzog, S. P., Ward, A. S., Wondzell, S. M., Serchan, S. P., González-Pinzón, R., & Zarnetske, J. P. (2025). Seasonality controls biogeochemical shifts in oxygen, carbon, and nitrogen along a 12-m, 54 hr-long hyporheic flowpath. *Water Resources Research*, *61*, e2024WR038410. https://doi.org/10.1029/2024WR038410

Received 30 JUL 2024
Accepted 27 MAR 2025

Abstract Hyporheic exchange is critical to river corridor biogeochemistry, but decameter-scale flowpaths (~10-m long) are understudied due to logistical challenges (e.g., sampling at depth, multi-day transit times). Some studies suggest that decameter-scale flowpaths should have initial hot spots followed by transport-limited conditions, whereas others suggest steady reaction rates and secondary reactions that could make decameter-scale flowpaths important and unique. We investigated biogeochemistry along a 12-m hyporheic mesocosm that allowed for controlled testing of seasonal and spatial water quality changes along a flowpath with fixed geometry and constant flow rate. Water quality profiles of oxygen, carbon, and nitrogen were measured at 1-m intervals along the mesocosm over multiple seasons. The first 6 m of the mesocosm were always oxic and a net nitrogen source to mobile porewater. In winter, oxic conditions persisted to 12 m, whereas the second half of the flowpath became anoxic and a net nitrogen sink in summer. No reactive hot spots were observed in the first meter of the mesocosm. Instead, most reactions were zeroth-order over 12 m and 54 hr of transit time. Influent chemistry had less impact on hyporheic biogeochemistry than expected due to large amounts of in situ reactant sources compared to stream-derived reactant sources. Sorbed or buried carbon likely fueled reactions with rates controlled by temperature and redox conditions. Each reactant showed different hyporheic Damköhler numbers, challenging the characterization of flowpaths being intrinsically reaction- or transport-limited. Future research should explore the prevalence and biogeochemical contributions of decameter-scale flowpaths in diverse field settings.

Plain Language Summary Water quality changes during the flow of water from a stream into the streambed and then back to the stream ("hyporheic exchange"). Decameter-scale (~10 m long) hyporheic flowpaths are understudied because of logistical challenges; we don't know if they are more or less efficient than shorter flowpaths at changing water quality. We made a 12-m model hyporheic zone ("mesocosm") from aluminum pipes filled with streambed sediments. We pumped stream water into the mesocosm and measured changes in oxygen, carbon, and nitrogen along the flowpath over different seasons. During winter, the entire mesocosm had high levels of oxygen and released nitrogen, while in summer, the oxygen was consumed in the first 6 m and subsequent low oxygen levels allowed bacteria in the mesocosm to remove nitrogen. Most reactions were constant along the flowpath because there was a lot of carbon and nitrogen in the streambed sediment. These internal sources of nutrients mattered more than the nutrients in the incoming stream water, but temperature and oxygen levels were also very important. Reactants were used up at different rates, meaning a flowpath can simultaneously be too long, too short, and optimal for water quality changes. More field research should explore decameter-scale hyporheic flow and stream water quality.

1. Introduction

Hyporheic exchange includes a nested array of flowpaths with broad ranges of transit times and geometries (Buffington & Tonina, 2009; Wondzell et al., 2022). The shortest (<2 m) and fastest (<24 hr transit time) hyporheic flowpaths are the easiest and most frequently monitored and, therefore, are the basis for most of the process-based understanding of hyporheic zones and how they control water quality dynamics along river

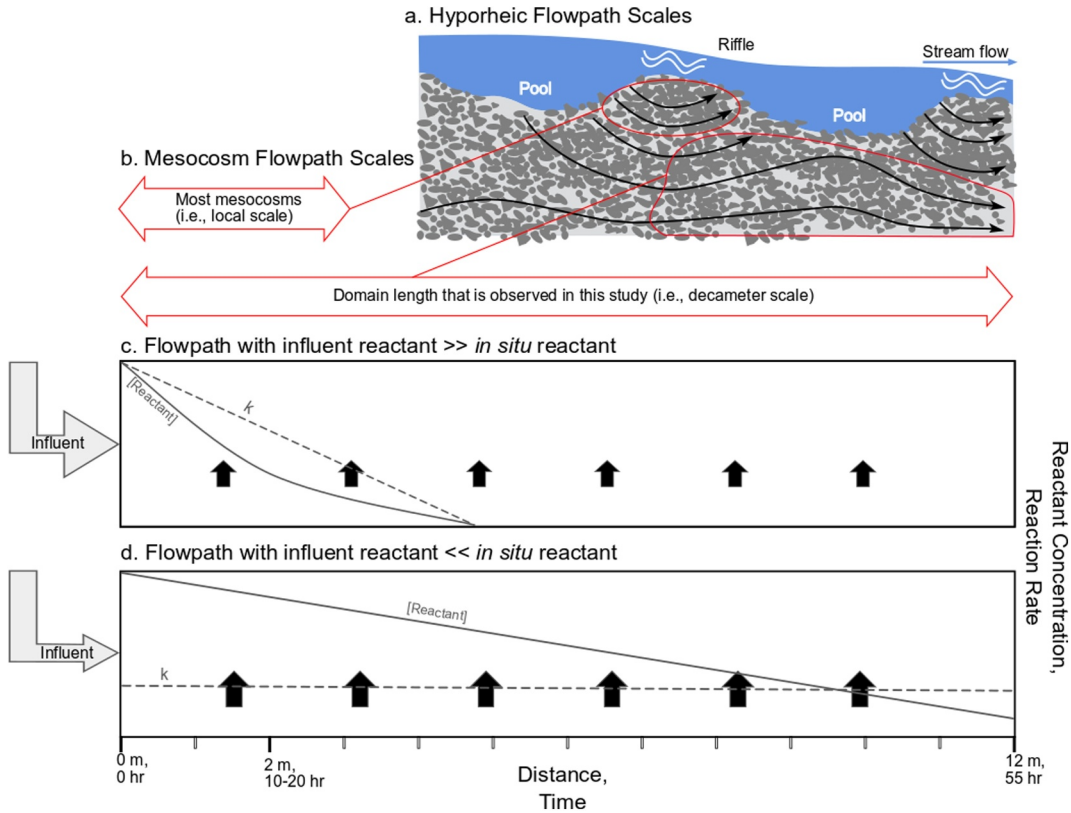

Figure 1. Conceptual representation of local-scale hyporheic flowpaths versus decameter-scale hyporheic flowpaths (Panel a; adapted from Wondzell et al., 2022) and corresponding mesocosm lengths in this study and other studies (Panel b). Two different end-member patterns have been proposed for decameter-scale flowpath biogeochemistry (Panel c) initial hot spots followed by transport-limited conditions, or (Panel d) slow reaction rates and continual reactant sources fuel continuous reactions. These end-member patterns diverge much more clearly in a 12-m mesocosm compared to prior ∼2-m mesocosm studies. Gray arrows represent influent reactant sources, black arrows represent in situ reactant sources, and the size of the arrow is proportional to the source flux. The diagram is conceptual and not to scale.

corridors (Ward, 2016; Ward & Packman, 2019). However, field (e.g., Gooseff et al., 2003; Payn et al., 2009) and modeling (e.g., Schmadel et al., 2017) studies show that substantial hyporheic exchange occurs over longer time scales (>24 hr transit time) due to longer flowpath lengths (>2m) or slower hyporheic flow velocities (Figure 1). In this work, we refer to these understudied longer spatial-scale and time-scale flowpaths as decameter-scale (i.e., 10–100 m in length) to differentiate them from the more studied local-scale flowpaths (i.e., ∼1 m), reach-scale (i.e., ∼100 m) hyporheic exchange, and regional-scale (∼1,000 km) groundwater interactions (Blöschl & Sivapalan, 1995). Decameter-scale flowpaths typically correspond with intermediate-scale flowpaths (after Tóth, 1963) that span multiple hyporheic structures in headwater systems (Herzog et al., 2019), although we acknowledge that >24 hr transit times can also be observed over sub meter-scale lengths (e.g., 88 hr in 15 cm; Harvey et al., 2013) and decameter-scale flowpaths can also be local-scale when studying large features such as meanders (e.g., 31 m flowpath; Peterson & Sickbert, 2006). In other words, space-time correlations will not be constant across systems, but decameter-scale is a useful heuristic to describe hyporheic flowpaths between local and reach scales.

What contributions do decameter-scale flowpaths make to hyporheic biogeochemistry? For a given influx of stream water, the biogeochemical function of a hyporheic flowpath of any scale will depend primarily on transit time and sediment reactivity (Gu et al., 2007; Harvey et al., 2013; Herzog et al., 2023; Zarnetske et al., 2012). Decameter-scale flowpaths often have multi-day hyporheic transit times that indicate potential for substantial reaction progress. However, sediment reactivity is difficult to predict due to spatial variation along individual flowpaths (i.e., as reactants and products are used or formed) and across flowpaths that pass through heterogeneous sediments and biofilms (Arnon et al., 2007; Battin et al., 2003; Boano et al., 2014; McClain et al., 2003;

Roy Chowdhury et al., 2020; Sawyer, 2015). Temporal fluctuations in physical conditions (e.g., head gradients, permeability, ice; Peter et al., 2019; Schmadel et al., 2017; Ward et al., 2018b; Zarnetske et al., 2008), chemical conditions (e.g., influent concentrations and temperatures; Hampton et al., 2019; Marzadri et al., 2013), biological conditions (e.g., macro-invertebrates; Lowell et al., 2009; Mermillod-Blondin et al., 2003), and microbial community structure and function (Nelson et al., 2020; Rutere et al., 2020) make the total biogeochemical function of a flowpath difficult to quantify, even for short and rapid flowpaths (Lewandowski et al., 2011), but particularly for larger-scale flowpaths.

Despite the aforementioned examples of heterogeneities in sediment reactivity, two consistent patterns have emerged from empirical study of hyporheic biogeochemistry. First, many studies report higher reaction rates at the start of hyporheic flowpaths that decline along the flowpath length, either consistently over time or seasonally (i.e., hot spots and hot moments after Krause et al., 2017; McClain et al., 2003). These observations suggest that decameter-scale flowpaths will be less efficient or transport-limited as stream-sourced reactants are exhausted (Harvey et al., 2013; riffle location in Pusch, 1996; Roy Chowdhury et al., 2020; Sobczak & Findlay, 2002). In contrast, other studies have observed relatively uniform reaction rates along hyporheic flowpaths (Corson-Rikert et al., 2016; pool location in Pusch, 1996; Serchan et al., 2024) or secondary reactions requiring longer activation transit times (e.g., Hampton et al., 2020; Quick et al., 2016). In these reaction-limited conditions, in situ reactant sources or cascading redox reactions can fuel nutrient cycling along the full flowpath length (e.g., transit times of tens of hours), indicating that decameter-scale flowpaths provide important, and perhaps different, biogeochemical functions compared to shorter time-scale flowpaths.

The relevance of decameter-scale flowpaths to hyporheic biogeochemistry depends on whether nutrient cycling reactions along a flowpath are mainly fueled by dissolved organic carbon (DOC) and other stream-derived constituents (Figure 1c) or by in situ sources within streambed sediments (Figure 1d), such as buried particulate organic carbon (POC), biofilms, and sorbed organic matter (e.g., Battin et al., 2003; Findlay et al., 1993; Jardine et al., 1992; Weigner et al., 2005). The availability of carbon within these systems is inherently complex and challenging to predict, as the spatiotemporal variability of DOC versus in situ carbon contributions can influence the rates and locations of biogeochemical processes (Brugger, Reitner, et al., 2001; Sobczak et al., 1998). This variability affects microbial activity, nutrient cycling, and oxygen dynamics, creating dynamic feedbacks that define the net functioning of hyporheic zones. Despite its importance, relatively few studies have explicitly examined the relative roles of DOC versus in situ carbon in streambed sediments along well-characterized field or mesocosm flowpaths while simultaneously measuring key parameters such as bulk DOC, dissolved oxygen (DO), and POC mass fraction. Several experiments demonstrated that DOC is a stronger control on hot spot formation and hyporheic metabolism than in situ carbon (e.g., Jones et al., 1995; Sobczak & Findlay, 2002). While these studies have explored a relatively wide range of DOC concentrations (i.e., approximately 1–8 mg C/L) they were limited to streambed systems with sediment organic carbon percentages $\leq$1%. Conversely, studies emphasizing the role of POC in hyporheic metabolism have reported POC ranging from 1% to 3% but these higher amounts of in situ carbon were also paired with elevated DOC (i.e., 3–10 mg C/L), did not isolate individual flowpaths (Brugger, Reitner, et al., 2001; Hedin, 1990; Sobczak et al., 1998), or had other confounding factors such as the use of irrigation with artificial groundwater (Gu et al., 2007) or investigation of non-streambed environments such as lakebeds (Hampton et al., 2019). Serchan et al. (2024) tested hyporheic mesocosms with 3% sediment organic carbon and seasonally variable DOC concentrations of approximately 0.5–2.5 mg C/L. These experiments revealed zeroth-order oxygen consumption, with an average of 83% attributed to in situ carbon. However, these results were confined to 2-m flowpath lengths with 1-m spatial resolution and from a hyporheic well field that did not adequately isolate flowpaths and may have been subject to re-aeration (Corson-Rikert et al., 2016; Serchan et al., 2024). Further research is needed to determine whether the patterns apparent in Serchan et al. (2024) can be confirmed at longer spatial scales while also testing the controls on decameter-scale flowpath biogeochemistry over multiple seasons.

There are numerous challenges to the empirical study of the controls on reaction-versus transport-limited conditions, especially along decameter-scale flowpaths. The spatiotemporal heterogeneities in sediment reactivity and hyporheic transit times, described above, are amplified in decameter-scale flowpaths that integrate additional spatial variability, require longer experimental durations, and show greater sensitivity to temporal fluctuations in hydraulic head gradients (Herzog et al., 2019; Schmadel et al., 2017). For example, decameter-scale flowpaths are often left unresolved in field tracer studies and are instead considered to be gross gains or gross losses (Payn et al., 2009) because their timescales exceed windows of detection for common tracer tests (Harvey &

Wagner, 2000; Ward et al., 2013, 2023). Recent efforts to overcome the challenges in spatiotemporally variable and interacting controls focus on improved experimental design in field settings, reducing complexity with controlled laboratory experiments, or numerical modeling. However, most field studies report site- and season-specific findings with little ability to control for dynamic flowpath geometry, transit times, temperatures, and initial nutrient concentrations. Several studies are empirically comprehensive (e.g., Corson-Rikert et al., 2016; Zarnetske et al., 2011a) but are limited to a single replicate in time or account for only a subset of processes (e.g., omitting mixing between flowpaths; Hester et al., 2017). Other empirical studies (Hampton et al., 2019, 2020; Peter et al., 2019) isolate a single downwelling flowpath but cannot control for mixing or mass losses. While laboratory studies assessing reaction rates in batch studies or small columns (e.g., Liu et al., 2017; Navel et al., 2011) are much more replicable, they do not account for the full complexity of spatiotemporal variations along natural flowpaths.

How, then, can we balance the dynamics and heterogeneity of natural hyporheic processes with our desire to control for confounding factors like changes in flowpath geometry, advective flow rate, and inclusion of relevant physical and biogeochemical conditions? A streamside hyporheic mesocosm (i.e., multiple meters of conduit packed with hyporheic sediment and irrigated with ambient stream water over multiple seasons) is a reasonable compromise between field complexity, controlled laboratory experiments, and physically based modeling. With a mesocosm setup, important hydraulic parameters such as flowpath length, mechanical dispersion, and sediment characteristics can be held constant. Some mesocosm studies also control porewater velocities and transit times to isolate additional reaction variables (Serchan et al., 2024). These controlled systems can isolate the effects of influent water quality (e.g., DO, DOC, temperature) on shifts in hyporheic biogeochemistry. However, most mesocosm studies only consider short flowpaths of ≤2 m (e.g., Serchan et al., 2024) or use idealized or fixed influents (e.g., Hampton et al., 2019, 2020). We are unaware of any field or mesocosm study of clearly defined hyporheic flowpaths of greater than 4 m (or timescales >40 hr) and operated over many months and seasons. Further, the limited number of studies that delineated hyporheic flowpaths have all remained oxic along the observed flowpath lengths, preventing investigation of the anoxic transition.

Our objective in this study was to quantify the controls on transport-versus reaction limitation (Harvey et al., 2013) for multiple key constituents in a decameter-scale hyporheic flowpath. Specifically, we asked.

1. How variable is DO, N, and C biogeochemistry between summer and winter, given natural variation in both influent reactant loads and temperature? We expect seasonal water temperature and organic carbon availability to control aerobic respiration rates and the timing and location of oxic-anoxic transitions.
2. How variable is DO, N, and C biogeochemistry along a fixed-geometry, 12-m flowpath? We expect to identify the most rapid transformations (i.e., hot spots) of all three reactants at the upstream (or proximal end) of the flowpath, where influent concentrations are highest, compared to the downstream (or distal end) of the flowpath.

To answer these questions, we monitored water temperature, DO, C, and N in a streamside mesocosm through an annual cycle in a catchment experiencing significant seasonal changes. Our mesocosm was held constant with respect to flowpath geometry, transit times, sediment characteristics, and transport processes, enabling us to isolate the role of influent and in situ reactant sources on hyporheic reactivity dynamics at spatiotemporal scales previously unexplored.

2. Materials and Methods

2.1. Site Description

The mesocosm facility is located adjacent to the stream gauge of Watershed 1 (WS01), a 2nd-order mountain stream in the H.J. Andrews Experimental Forest (44.20741 N, 122.25831 W). The 96-ha watershed is drained by a steep (~12% gradient) cobble and gravel-bedded stream that flows over a series of step-pool sequences formed by logs and boulders. Stream water was pumped directly from WS01 and into the mesocosm (construction and operation details below). Long-term data sets on flow, temperature, electrical conductivity, sediment transport, and other water quality parameters are described in Johnson et al. (2021) and specific data sets for WS01 are available from the H.J. Andrews data bank. In WS01, continuous stream gauging started in 1952 and stream chemistry sampling started in 2003 with flow-proportional water samples composited over 3-week intervals. Specific date ranges cited in the present study are provided below. Notable seasonal fluctuations in WS01 stream water that were expected to influence hyporheic biogeochemical function included temperature, discharge, and

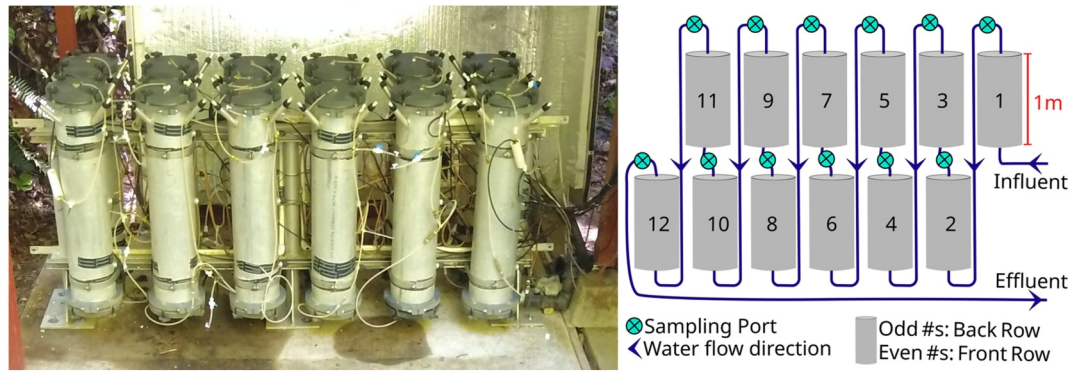

Figure 2. Photo (left) and schematic (right) of mesocosm system with 12 different 1-m long columns connected in series. Half of the insulated aluminum shell is also visible in the background (left).

DOC. Average water temperatures varied from approximately 4–6°C in the winter to 15–17°C in the summer (Database Code HT004 for 1997–2019; Gregory & Johnson, 2019), while discharge varied from winter baseflows of approximately 90 L/s in December-January to summer baseflows of <1.5 L/s in July-August (Database Code HF004 for 1953–2019; Johnson et al., 2024). WS01 typically becomes spatially intermittent during summer low flows (Ward et al., 2018a, 2020). Average stream DOC peaked at ∼2.0 mg/L in late October-November due to allochthonous inputs of deciduous leaf litter and declined to an annual low of ∼1.0 mg/L in late July–August (Database Code CF002 for 2004–2018; Johnson & Fredriksen, 2019). Seasonal inputs of allochthonous carbon are widely known to stimulate stream (e.g., Findlay & Arsuffi, 1989) and hyporheic zone (e.g., Argerich et al., 2011) metabolism. This experiment tests the impacts of these consistent seasonal shifts on the biogeochemistry of a fixed-geometry mesocosm flowpath.

2.2. Mesocosm Materials and Construction

Mesocosm schematics and construction methods are detailed in Serchan (2021) and Serchan et al. (2024). In brief, the mesocosm (Figure 2) consisted of 12 connected aluminum pipes (length = 1 m, internal diameter = 0.203 m). Water flowed into and out of each pipe segment via a small port in each endcap, and the pipe segments were connected in series with polyethylene tubing (inner diameter 0.0043 m). To convert point source inputs and outputs into uniform plug flow, each end cap was designed with a 40 μm sintered stainless steel mesh diffuser plate inserted between the sediment and the HDPE end caps, which were machined with a series of radial grooves to spread flows laterally as they enter the pipe and collapse them back to the exit point. To keep the sintered stainless-steel mesh diffuser plate from clogging, the stream water was pumped through a series of progressively finer stainless-steel filters with nominal pore sizes of 500, 150, and 50 μm.

Each 1-m pipe was packed with native streambed sediment sourced from a bed load sediment collection basin about 50 m downstream from the WS01 gauge. Sediment was sieved through square 6-mm openings to exclude large particles that would create preferential flow paths within the pipe segments. Thus, rocks and large pieces of organic material were removed from the sediment (Serchan, 2021). Sieved sediment was homogenized, distributed evenly across each 1-m pipe, and compacted, with a resulting porosity of 40.4%. In each of the 12 mesocosm pipes, the pore volume was approximately 13.1 L out of the total volume of 32.4 L. Particulate organic carbon constituted 3% of the mass of the dry sediment in the mesocosms based on loss on ignition analyses (Serchan et al., 2024). The sediment bulk density for the mineral solids was assumed to be 2.57 g/cm^3 (average of local parent geologic materials - andesite and basalt).

Pipes were mounted vertically, and water was pumped upwards from the bottom of one pipe to the outlet at the top and then into the bottom of the next pipe. The entire assembly was enclosed in an insulated aluminum shell that could be removed for sampling. To mitigate the difference between air and stream water temperatures, ambient stream water was continuously circulated through a copper pipe radiator within the insulated shell. Two electric heat cables were also used during winter to prevent the mesocosm from freezing.

Pairs of pipe segments were connected and packed with streambed sediment in May 2016 to create six mesocosms, each with a 2-m flowpath (Serchan et al., 2024). In April 2019, the pipe segments were connected to form a

Table 1
Dates and Locations of Mesocosm Sampling

	DO profiles	Water chemistry samples
Number of Sampling Points	$N_p = 13$; 1 influent and 12 every 1 m	$N_p = 13$; 1 influent and 12 every 1 m
2019 Sampling Dates	$N_s = 7$; MAY 31, JUN 21, JUL 31, OCT 31, NOV 11, DEC 03 and 16	$N_s = 1$; DEC 16
2020 Sampling Dates	$N_s = 11$; JAN 20, FEB 03, MAR 03, MAY 01, JUN 29, JUL 02 and 15, AUG 03, 10, 13 and 18	$N_s = 1$; AUG 18

Note. N_p = number of ports sampled each date and N_s = number of sampling dates.

single 12-m flowpath. The first and second pipe segments of each 2-m mesocosm were alternated to prevent potential systematic differences along the 12-m mesocosm. The pipe segments were not repacked with fresh sediment before this flowpath reconfiguration. Thus, initial conditions in April 2019 did not necessarily reflect the conditions expected with increasing length and residence time of water along the length of a 12-m flow path. Hence, the mesocosm was left to re-equilibrate to these new decameter-scale flowpath conditions for approximately 6 weeks before collecting the first DO measurements for this study, and the first water samples were collected more than 7 months after reconfiguring the mesocosm to the single 12-m long flowpath.

Stream water was pumped through the mesocosm continuously from May 2016 through August 2020. A submersible electric pump was used to raise ambient stream water to a head box located 3 m above the mesocosm inlet to maintain a constant inlet pressure for the mesocosm. The level of the mesocosm outlet was fixed to provide a constant head gradient, and a high-precision valve at the mesocosm outlet controlled the flow rate through the mesocosm.

Flow was maintained at 48 mL/min during the study period, but fluctuations of up to 20% were common between manual adjustments to the flow rate. Preliminary experiments showed that the flow rate of 48 mL/min generated a transit time of 4.54 hr for each column or 54.48 hr for all 12-m. Flow dropped at times to <20 mL/min due to filter clogging after storm events but was manually restored to 48 mL/min within 24–72 hr after storms. After any storm event, the mesocosm was returned to ambient conditions for several days before any new DO profiles or water quality samples were collected.

2.3. Sampling Protocol and Handling

DO and temperature profiles were monitored on 18 dates between May 2019 through August 2020 (Table 1). Our goal was to monitor DO and temperature profiles approximately once per month to capture a wide range of seasonal conditions, but the actual frequency of monitoring varied based on personnel availability and access conditions for this remote site. Grab samples to monitor profiles of C and N along the mesocosm were collected in December 2019 (hereafter referred to as winter samples) and August 2020 (hereafter referred to as summer samples) to provide more comprehensive biogeochemical analyses at time points when the DO and temperature profiles were at or near the maximum seasonal differences. Mesocosm monitoring ceased abruptly due to the Holiday Farm Fire, which burned from September through October 2020, cutting off personnel access and electrical power to the mesocosm facility.

DO and temperature were measured with a handheld YSI ProODO probe. A flow-through sampling chamber was affixed to the sampling port between each mesocosm column, and the DO probe was submerged in the chamber and allowed to equilibrate.

All mesocosm sampling (i.e., grab samples) started at the downstream end of the mesocosm ($x = 12$ m) and worked upstream toward the mesocosm inlet ($x = 0$ m) to minimize the interference of sampling on water quality. We sampled at the ambient flow rate from tubing that connects each pipe segment rather than pumping from the porewater because pumping may disturb the ambient flow conditions. Sampling at the ambient flow rate took several hours, but this was less than the mean travel time of a single pipe segment.

Water samples for DOC, NH_3, $NO_3 + NO_2$, and total dissolved nitrogen (TDN) were collected in acid-washed 250 mL HDPE Nalgene® bottles. Dissolved inorganic carbon (DIC) samples were collected unfiltered in acid-washed 60 mL BD® syringes. Samples were stored on ice upon collection and then delivered to the Cooperative Chemical Analytical Laboratory (CCAL) in Corvallis, Oregon, within 24 hr of collection. At CCAL,

unfiltered DIC was analyzed within 24 hr. Filtered DOC aliquots were separated, refrigerated, and analyzed within 48 hr for the winter sample but within 60 days for the summer sample. The remaining filtered samples were frozen for less than 60 days before being thawed and analyzed. Carbon samples were then analyzed using a Shimadzu TOC-VSCH Combustion Carbon Analyzer. NH_3, NO_3 + NO_2 were analyzed via Lachat QuikChem 8,500 Flow Injection Analyzer, while TDN was analyzed by Technicon Auto-Analyzer II.

2.4. Calculations and Data Analyses

All analyte profiles were assessed using the MATLAB linear model function *fitlm*(), which generates a linear slope intercept model with R^2, RMSE, and outputs standard error for the *y*-intercept and slope. To determine which analyte profiles had significant spatial trends along the 12-m mesocosm, we considered any slopes that included zero within slope ± one standard error to be not significantly different from zero. To test for significant differences between summer and winter reaction rates and oxic-anoxic portions of the mesocosm, we considered any models that had overlap between their slopes ± one standard error to be not significantly different. However, we also noted where significant relationships had such small slope values that they were unimportant. The number of significant figures reported in measurements and calculations varies according to the original measurement instruments. For example, water temperature was measured to the tenth of a degree Celsius, whereas nitrogen was measured in mg N/L to the thousandth place.

All analyte profiles were modeled as both zeroth- and first-order reactions. Because both reaction orders tended to provide similar R^2 values, we proceeded with zeroth-order models unless R^2 values were at least 10% higher for first-order models or if visual inspection showed that first-order reaction rates were more appropriate than indicated statistically (e.g., where first-order rates for denitrification have 0%–10% higher R^2 but better match the shape of the profile). We clearly describe any places where first-order reaction kinetics are used.

The concentration of dissolved organic nitrogen (DON) was calculated as the difference between TDN and the sum of NH_3 + NO_3 + NO_2, where all analytes are reported in mg N/L.

3. Results

3.1. Seasonal Temperature Shifts Corresponded With Changes in Influent DO Concentrations, DO Consumption Rates, and Redox Boundaries

We observed seasonal fluctuations in the temperature and DO profiles through the 12-m mesocosm (Figure 3, Figure S1 in Supporting Information S1). Across 18 sampling dates, the average temperature of the mesocosm ranged from 4.5°C to 20.1°C. On any given date, there was a range of temperatures along the mesocosm (2.2°C ± 1.0°C, mean±SD) attributable to imperfect insulation (i.e., the air around the mesocosm did not exactly match the water temperature) and the propagation of the stream's diurnal temperature fluctuations through the multi-day mesocosm transit. The mesocosm tended to be colder than the stream in winter and warmer than the stream in summer, but fell within the observed range of stream temperatures within the WS01 gauge record (i.e., 0.2°C–23.2°C; H.J. Andrews Data set HT004 1997–2019; Gregory & Johnson, 2019). On sampling dates with average mesocosm temperatures above 11.0°C (n = 11; Figure 3), the mesocosm always developed anoxic conditions (i.e., DO < 2 mg/L) by the end of the 12-m flowpath. The shortest anoxic transition was at 6-m (i.e., at a 27-hr transit time), observed on the two warmest sampling dates. In contrast, on all sampling dates with average mesocosm temperatures less than 10.0°C (n = 7; Figure 3), the mesocosm remained oxic along the full 12-m flowpath (i.e., after 54-hr of transport). Thus, the location of the oxic-anoxic boundary varied seasonally by at least 6 m.

Oxygen consumption rates were generally best represented by zeroth-order reaction kinetics with R^2 of 0.86 ± 0.19 (mean ± st. error; Figure S1 in Supporting Information S1) across the 18 profiles, although first-order reaction kinetics also matched observed data well (R^2 of 0.85 ± 0.14; Figure S1 in Supporting Information S1). However, visual inspection showed that the zeroth-order models better aligned with the observed DO concentrations across the oxic portion of the profiles, only deviating from observations when DO dropped below 2 mg/L. A breakpoint applied at DO < 2 mg/L indicated that while zeroth-order kinetics represented the initial reaction rate well, DO profiles changed slope and became less linear below the 2 mg/L oxic-anoxic boundary (Figure S1 in Supporting Information S1). Restricting the initial reaction rate calculation to observations where DO > 2 mg/L improved R^2 to 0.99 ± 0.01. In particular, the lowest R^2 values on the two warmest sampling dates (19.8 and

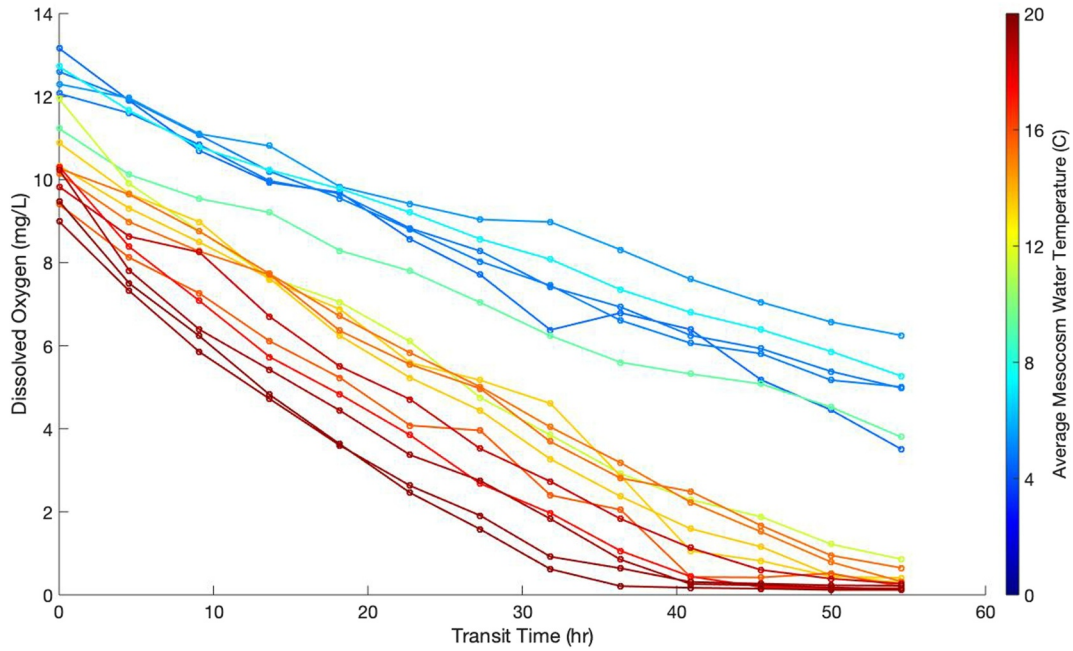

Figure 3. DO profiles versus transit time through the 12-m mesocosm. The profiles (n = 18) span 16 months and multiple seasons. Each profile's color reflects the average water temperature in the mesocosm during sampling. See individual profiles by date in Figure S1 in Supporting Information S1.

20.1°C) improved from 0.44 to 0.50, respectively, to 0.99 for both dates when the anoxic data points were considered separately.

Increasing influent temperatures were highly correlated with decreasing influent DO concentrations (R^2 = 0.88; Figure S2 in Supporting Information S1), and increasing mesocosm temperatures were highly correlated with increasing oxygen consumption rates (R^2 = 0.80). Across 18 oxygen profiles, influent DO was up to 32% lower during warm periods than cold periods (9.0 vs. 13.2 mg/L, respectively), and DO consumption rates were up to 2.7 times faster (−0.30 vs. −0.11 mg/L/hr). Dissolved oxygen consumption rates along oxic portions of the flowpath can be explained by temperature according to several models, including a linear regression (R^2 = 0.80), exponential regression (R^2 = 0.82), or the Arrhenius equation (R^2 = 0.80; using the average temperature and average reaction rate as the reference point and Θ = 1.043, within the common range of 1.02–1.06 for BOD after Siegrist, 2016) (Figure S3 in Supporting Information S1).

The largest and smallest influent DO concentrations (13.2 and 9.0 mg/L) occurred during the winter and summer, respectively, and occurred on the same dates that we collected water chemistry samples for C, N, O. For oxic portions of the mesocosm, DO consumption rates were approximately 50% higher during summer (−0.25 mg/L/hr) than in winter (−0.16 mg/L/hr). During summer sampling, the mesocosm crossed the anoxic threshold at 6 m (i.e., DO = 1.91 mg/L at 27-hr transit time) and was well below the threshold by 7 m (i.e., 0.92 mg/L at 32-hr transit time). The slope break in oxygen consumption rate was especially pronounced at x = 7 m, where the rate declined substantially whether modeled as a zeroth-order reaction rate of −0.03 mg/L/hr (R^2 = 0.80) or a first-order reaction rate (−0.07 hr^{-1}; R^2 = 0.87). Therefore, we used x = 7 m as the functional oxic-anoxic boundary for the summer sampling date.

3.2. Seasonal Shifts in Influent Concentrations and Transformation Rates of Carbon and Nitrogen Occurred, But Spatial Heterogeneity Was Only Observed at the Oxic-Anoxic Boundary

3.2.1. Carbon Responses to Seasonal Shifts

Our samples showed that the stream water entering the mesocosm had 127% more DOC in winter than in summer (influent at 1.66 vs. 0.73 mg/L), whereas influent DIC was 60% higher in summer than in winter (influent at 7.58 vs. 4.73 mg/L; Figure 4). For DOC transformation rates, the zeroth-order models performed equal to, or slightly

better than, the first-order models (Tables S1–S8 in Supporting Information S1). The zeroth-order DOC consumption rate was 3.2 times higher in winter (k_{DOC} = −0.0092 mg/L/hr; R^2 = 0.87) than in summer (k_{DOC} = −0.0022 mg/L/hr; R^2 = 0.58) despite much colder winter temperatures. DIC production along the mesocosm was also approximately zeroth-order and was lower in winter (k_{DIC} = 0.0316 mg/L/hr; R^2 = 0.97) than the average across the full mesocosm in summer (k_{DIC} = 0.0383 mg/L/hr; R^2 = 0.88). However, the summer DIC production was even higher in the oxic portion of the mesocosm before slowing significantly under anoxic conditions (oxic k_{DIC} = 0.057 mg/L/hr vs. anoxic k_{DIC} = 0.014 mg/L/hr).

DIC generation consistently exceeded net losses in DOC along the mesocosm flowpath, even during winter when influent DOC and k_{DOC} were elevated. The partial decoupling of DIC generation from DOC consumption was pronounced, with the ratio of k_{DIC}/k_{DOC} reaching 17.4 during summer sampling due to a higher k_{DIC} and lower k_{DOC} than in winter (winter k_{DIC}/k_{DOC} = 3.4). Net DIC flux from the mesocosm followed similar ratios, with DIC production 17.5- and 3.4-fold higher than DOC consumption in summer and winter, respectively. DOC attenuation and DIC production rates did not vary along the mesocosm in winter, but both slowed in summer within the anoxic portions beyond 7 m (i.e., at transit times >32 hr).

3.2.2. Nitrogen Responses to Seasonal Shifts

The TDN concentration in stream water entering the mesocosm during the summer sampling was 33% higher (0.08 mg N/L) than in the winter sample (0.06 mg N/L; Figure 4). In summer, the stream water concentration of $NO_3 + NO_2$ (0.051 mg N/L) was 410% higher than in winter (0.010 mg N/L), and the concentration of NH_3 was 75% higher than in winter (0.014 vs. 0.008 mg N/L, respectively). However, in winter, the stream water sample had 180% more DON. In total, DON comprised 70% of the nitrogen in the winter sample but only 19% in the summer sample.

Total dissolved nitrogen increased along oxic portions of the mesocosm flowpath during both winter (full 12-m flowpath, 54-hr transit time) and summer (first 7 m of the flowpath, 32-hr transit time), indicating the production of dissolved nitrogen from microbial processing of in situ sources. Increased TDN along oxic portions of the mesocosm was primarily driven by steady increases in $NO_3 + NO_2$, as NH_3 and DON concentrations were highly variable but had no meaningful trends in either season (i.e., all rates were not statistically significant or had absolute values <0.0003 mg N/L/hr). Zeroth-order production rates of TDN and NO_3+NO_2 along the oxic portion of the flowpath (both 0.0014 mg N/L/hr; R^2 = 0.58 and 0.94, respectively) were 170% and 75% higher in summer than in winter (0.0005 and 0.0008 mg N/L/hr, respectively, with respective R^2 = 0.66 and 0.91). However, the largest difference between seasons was the summer mesocosm shifting from net nitrate production to net nitrate removal, beginning with anoxic conditions at 7 m. While the $NO_3 + NO_2$ concentration continued to increase along the final meters of the mesocosm in winter, the summer concentration dropped to 0.0005 mg N/L, which was below the analytical limit of determination (i.e., 0.001 mg N/L for $NO_3 + NO_2$). From 8 to 12 m in the summer, the apparent removal rate for $NO_3 + NO_2$ was −0.005 mg N/L/hr for the zeroth-order model (R^2 = 0.83), but the first-order model performed better ($k = -0.263\ hr^{-1}$, R^2 = 0.97).

The oxic winter mesocosm was a net producer of DIN and a net source of N to the stream, with a positive net flux of 0.006 mg N/hr TDN and 0.010 mg N/hr $NO_3 + NO_2$. In winter, the influent accounted for 0.06 mg N/L, whereas in situ sources added 0.03 mg N/L, resulting in 0.09 mg N/L at the mesocosm outlet. The mesocosm shifted to a net denitrifying N sink in summer, consuming 0.070 mg N/hr each for TDN and $NO_3 + NO_2$. During summer sampling, the influent provided 0.08 mg N/L. At the 7m oxic-anoxic transition, TDN had risen to 0.14 mg N/L due to mobilization of in situ nitrogen sources, but TDN decreased to 0.03 mg N/L at the mesocosm outlet.

4. Discussion

4.1. What Drives Spatiotemporal Variability of DO, C, and N Biogeochemistry Along a Fixed-Geometry, 12-m Flowpath?

This study demonstrated a variable oxic-anoxic boundary (i.e., DO < 2 mg/L) along a fixed hyporheic flowpath with a constant flow rate, moving in space by more than 6-m during the study period. Anoxia developed over distances as short as 6 m (28 hr) during the warmest summer observations, but the DO concentrations remained above 6 mg/L at 12 m on colder sampling dates in the winter. Based on the slowest observed oxygen consumption rate, the flowpath is projected to remain oxic through 20 m of hyporheic flow. Unexpectedly, the moving seasonal

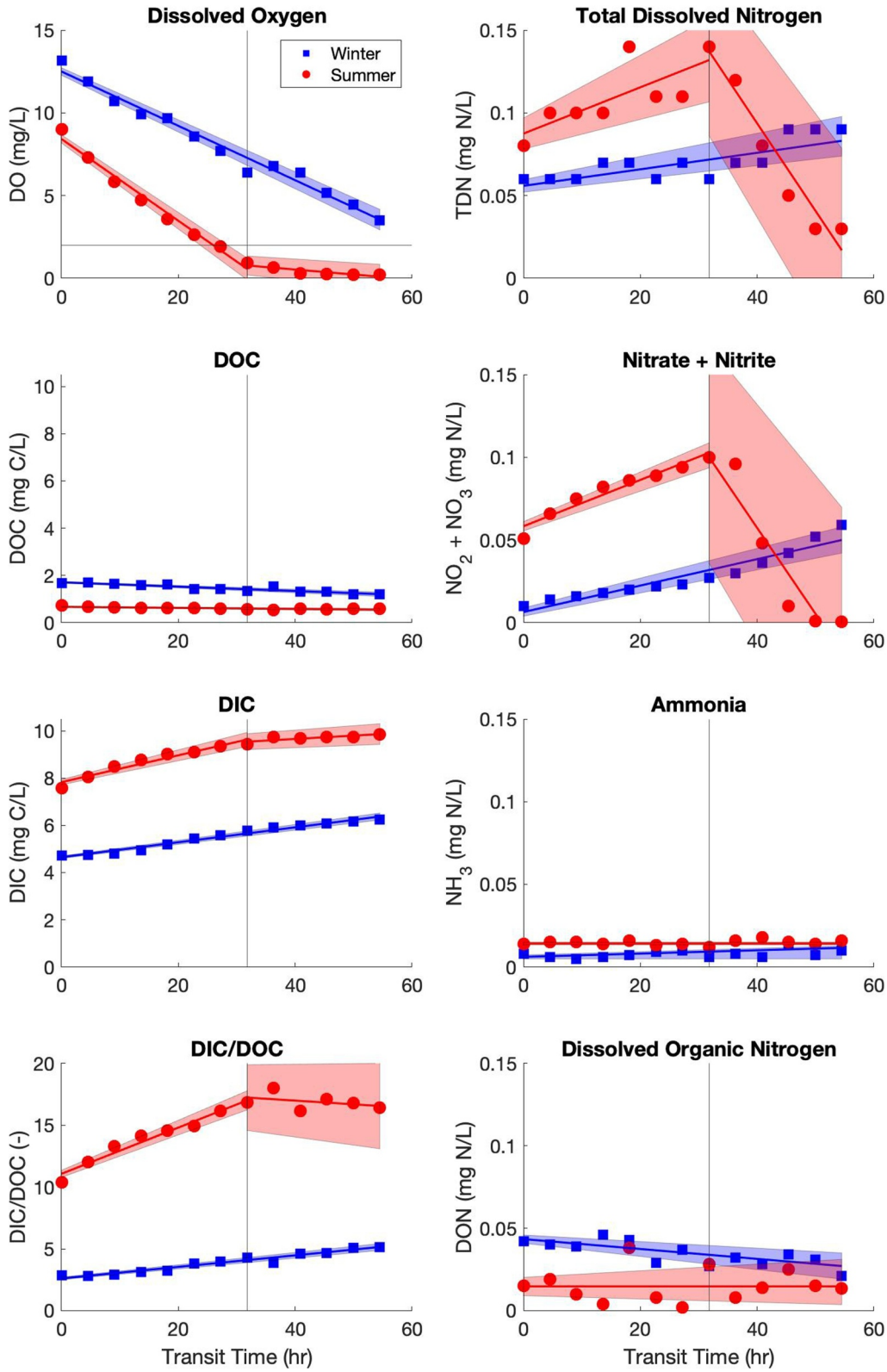

Figure 4. Profiles of DO, DOC, DIC, DIC/DOC, and nitrogen species during the winter (16-Dec. 2019) and summer (18-Aug. 2020) sampling events. Points show observed data, solid lines are linear best-fit models (i.e., zeroth-order), and shaded areas are 95% confidence intervals of linear models. The horizontal line at $y = 2$ mg/L DO (panel A) indicates the oxic-anoxic transition. The vertical line at $t = 32$ hr indicates the location $x = 7$ m where the mesocosm was bulk anoxic during summer.

redox boundary was the only significant source of spatial (but not temporal) variability in mesocosm reaction rates that we measured. In other words, all observed reaction rate constants were uniform (i.e., zeroth-order) over long distances and travel times (i.e., the entire mesocosm in winter, until the oxic-anoxic threshold in summer). Summer DOC and DIC reaction rates only slowed significantly when the bulk hyporheic water became anoxic, but they remained zeroth-order at the new, lower reaction rates. Oxic portions of the mesocosm were always net DIN sources due to the mineralization of organic N. However, once flowpaths became anoxic in summer, the more distal portions of the mesocosm then became a net sink for TDN. Under these anoxic conditions, nitrate was fully removed over the next 4 m (from 7-m to 11-m, representing 18.16 hr of travel time) of the flowpath and best represented as first-order decay. In sum, we observed seasonal expansion and contraction of the aerobic hyporheic zone, which was inversely correlated with denitrification. Our 1-D empirical results are similar to the 3-D simulations of a 4th-order stream and alluvial aquifer wherein the aerobic zone of hyporheic flowpaths was up to 6 times larger by volume in winter than in summer (Nogueira et al., 2021). In response to fluctuations in the oxic-anoxic boundary, denitrification zones also shifted from near-stream in summer to approximately 250 m from the stream in winter (Figure 9; Nogueira et al., 2021).

Reaction rates were more variable in space (along the flowpath in summer) than in time (summer vs. winter). Specifically, zeroth-order reaction rates for DO, DOC, DIC, TDN, and $NO_2 + NO_3$ differed by greater magnitudes when comparing the oxic and anoxic portions of the mesocosm in summer (i.e., first 7 m vs. last 5 m) than between the oxic portions of the mesocosm in summer versus winter. Reaction rates for NH_3 and DON differed equally between the same redox and seasonal shifts. Given the sensitivity of the observed biogeochemical parameters to redox zonation, it is critical but difficult to identify the underlying drivers of seasonal anoxia, as many parameters can be different between the broad categories of "summer" and "winter" seasons (Serchan et al., 2024). Indeed, we observed numerous seasonal variations in biogeochemical parameters that we expected to play important roles in hyporheic biogeochemistry (e.g., influent concentrations of reactants, temperature, and reaction rates). For example, winter DOC concentrations in the influent were more than twice the magnitude of summer DOC concentrations, consistent with historical records of allochthonous leaf litter inputs (Database Code CF002 for 2004–2018; Johnson & Fredriksen, 2019). Yet these seasonal differences in influent concentrations and temperatures had less direct influence on carbon and nitrogen cycling rates than did the summer redox shift.

We found that temperature alone can explain most temporal variations in DO profiles and, therefore, oxic-anoxic zonation. Specifically, water temperature was the key control on mesocosm DO profiles across 18 sampling dates by determining the influent DO concentrations ($R^2 = 0.88$) and the DO consumption rates ($R^2 = 0.80$). The DO in the influent water was always close to saturation because of fast reaeration along the step-pool morphology of WS01. However, temperature-dependent saturation concentrations were more than 4 mg/L lower in summer than in winter, and DO consumption rates were approximately 50% higher in summer than in winter. These results highlight the role of water temperature in driving hot spots and hot moments by altering reaction rates, in addition to solute concentrations and timescales that were the foci of McClain et al. (2003). In summer the mesocosm demonstrated rapid DO consumption followed by transport limitation (Figure 1c), yielding a redox shift and a denitrification hot spot. In winter, cold temperatures lowered reaction rates relative to DO supply, resulting in sustained slow oxygen consumption along the 12-m mesocosm (Figure 1d). Brugger, Wett, et al. (2001) also found that temperature was the best predictor of hyporheic DO concentrations, explaining at least 70% of the variance between points. Unlike the present mesocosm study, the sampling points in Brugger et al. were not along a single delineated flowpath and the remaining variance was attributed to differences between the numerous flowpaths sampled (e.g., hydraulic gradients, influent concentrations).

Since many experiments in mesocosms or carefully instrumented gravel bars have found higher reaction rates at the proximal ends of flow paths for DO, C, and N cycling, with hot spots occurring in the first 0.04–2.0 m (Harvey, B. N. et al., 2011; Harvey, J. W. et al., 2013; Knapp et al., 2017; Sobczak & Findlay, 2002; Sobczak et al., 2003; Zarnetske et al., 2011a), we expected that reaction rates would be higher in the first meter of the 12-m mesocosm than in subsequent sections. However, we saw little evidence of faster reaction rates occurring at the proximal end of the mesocosm. Instead, most reactions were well represented by zeroth-order reaction kinetics with a constant reaction rate along the entire flowpath, including all DO, C, and N reactions during winter sampling. As described above, the notable exceptions occurred when the mesocosm turned anoxic during summer sampling. Specifically, decreasing oxygen concentrations caused pronounced shifts to first-order kinetics in DO and nitrate consumption and lower magnitudes of zeroth-order rates of DOC consumption and DIC production. However, these new rates in the anoxic portion of the mesocosm were also constant along the remainder of the

flowpath and did not decrease with distance, indicating a lack of substrate limitation that is discussed in Section 4.2. The observed changes due to anoxia matched expectations in the literature for substrate-limitation causing shifts from zeroth-order to first-order reaction kinetics (e.g., Sheibley et al., 2003; Trauth et al., 2014), bulk anoxia as a control on nitrate source-sink behavior (Zarnetske et al., 2011b, 2012), and decreased DOC production (e.g., wood decomposition) rates under anoxic conditions (Fritz et al., 2006).

It is reasonable to consider whether our spatial sampling intervals were too coarse (i.e., 1 m; 4.54 hr transit time) to observe hot spots at the inlet of the mesocosm (e.g., in the first 0.04–0.30 m of the flowpath). However, the shapes of the solute profiles would make it difficult to impose faster reaction rates at the mesocosm inlets and still match the observed data at $x = 0$ and $x = 1$ m. Thus, even with a different mesocosm sampling design, we see little evidence that an initial biogeochemical hotspot could be present in our mesocosm and only observable with a different sampling design. Filtration of fine sediment and the lack of natural streambed processes (e.g., scour and deposition) in the mesocosm may also have contributed to the lack of observed hot spot behavior of the first meter of the mesocosm. However, during baseflow there tend to be few particulates in the stream water (Corson-Rikert et al., 2016), and most particles were smaller than the filter pore sizes (Serchan et al., 2024) such that the filtration system was unlikely to influence the pattern of reactivity we observed over the length of the mesocosm. Thus, the consistent trend of spatially uniform reaction rates we observed for DO, C, and N in the oxic portions of the mesocosm suggests that hotspots were not present at the inlet or along the flowpaths through the mesocosm.

The present study was also limited by a lack of experimental replicates. Serchan et al. (2024) studied six replicates of 2-m mesocosms and found that the variability between replicates decreased in proportion to effect size (i.e., change in solute concentration from inlet to outlet). Specifically, the coefficient of variation was 53% for O_2 (mean ΔO_2 = 2.43 mg/L), 75% for DIC (mean ΔDIC = 0.47 mg C/L), and 125% for DOC (mean ΔDOC = 0.10 mg C/L). Changes in the same constituents were generally 2- to 3-fold larger in the 12-m mesocosm than in the 2-m mesocosms, which would be expected to decrease the coefficients of variation compared to Serchan et al. (2024). Temporal replication of dissolved oxygen profiles over multiple seasons improves confidence in the findings, but cannot substitute for the lack of spatial replication of the entire system. Unfortunately, replicating the 12-m mesocosm was not possible due to logistical constraints, and dividing the system into triplicate 4-m mesocosms would have prevented us from observing decameter-scale flowpaths and the oxic-anoxic transition.

4.2. What Controls Transport-Versus Reaction-Limited Conditions for Multiple Constituents in Decameter-Scale Hyporheic Flowpaths?

The lack of observed hotspots in the first few meters of our mesocosm, as described above, raises the question of why variation in solute chemistry of influent stream water had little influence on hyporheic nutrient cycling. Based on the data collected in this study, the key difference in our mesocosm was likely the discrepancy between influent DOC fluxes versus in situ carbon stores. This case represents an example of the dynamic between reactants carried by influent water versus those already present throughout the substrate (Figure 5, after McClain et al., 2003). Specifically, hot spots followed by transport limitation are often observed when stream-derived reactants enter a hyporheic zone with relatively low in situ sources (Figure 5a). In contrast, we observed substantial in situ carbon and nitrogen sources relative to stream-derived components and relatively slow reaction rate constants, resulting in sustained reaction-limited conditions across oxic portions of the mesocosm (Figure 5b).

The relative amounts of stream-derived reactants versus in situ stored reactants differed between the present mesocosm study and many others. The stream water entering our mesocosm was oxygen-saturated but had relatively low DIN (i.e., <0.15 mg N/L) and DOC (i.e., <2 mg C/L) concentrations. Similar studies have reported DO concentrations between 7.5 and 8.3 mg/L, DOC between 1 and 8 mg C/L, and DIN between 0.01 and 10 mg N/L (Harvey et al., 2011, 2013; Sobczak et al., 2003; Sobczak & Findlay, 2002; Zarnetske et al., 2011a). Thus, the present study generally represents high DO and very low C and N concentrations compared to similar studies, although each parameter was still within the range of values reported in previous studies. Regarding in situ sources, large quantities of in situ carbon were present in the mesocosm sediment. The ~3% organic carbon by mass (even though large POC > 6 mm was excluded via sieving; Serchan et al., 2024) reported here is comparable to other forested sites (e.g., 1.3%–2.9% in Inwood et al., 2005) but much higher than in similar

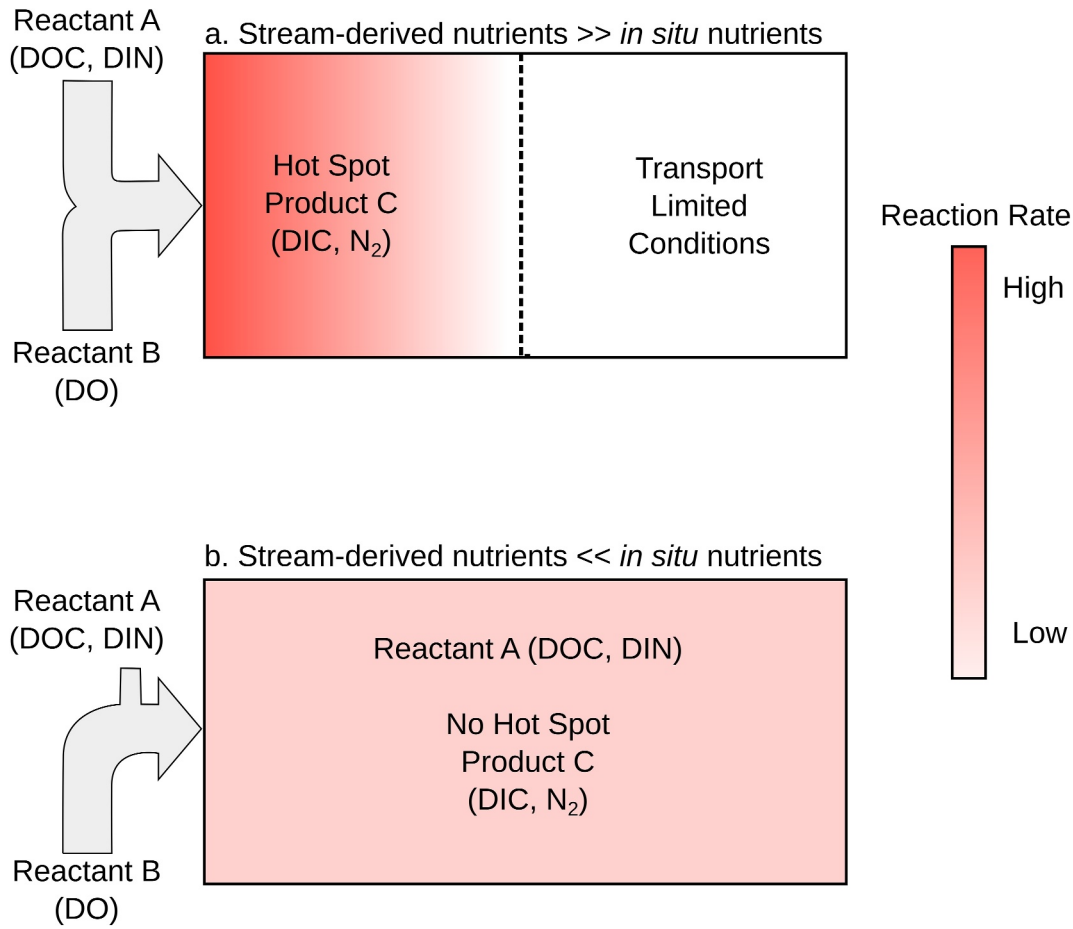

Figure 5. Conceptual representation of the role of stream-derived versus in situ reactant sources in hyporheic biogeochemistry, adapted from McClain et al. (2003). Note that a flowpath may be both reaction- and transport-limited for different solutes (i.e., DO, DOC, DIN) with different relative amounts of stream-derived versus in situ sources. In this study we also observed temperature-driven fluctuations in reaction rates that rapidly consumed in situ sources and shifted the 12-m mesocosm between patterns shown in Panel b (i.e., winter) and Panel a (i.e., summer).

hyporheic flowpath studies (Harvey et al., 2011, 2013; Sobczak et al., 2003; Sobczak & Findlay, 2002; Zarnetske et al., 2011a), both in terms of sediment content itself and as a ratio of sediment:stream carbon. For example, Harvey et al. (2013) reported stream water concentrations of DOC ranging from 3 to 5 mg C/L compared to only 0.2%–0.4% by mass of POC in the streambed sediment. Jones et al. (1995) and Valett et al. (1990) also studied a stream with DOC of 3 mg C/L and buried organic matter averaging only 0.08% by mass. Sobczak and Findlay (2002) instrumented gravel bars in five different streams in which DOC ranged from 1 to 8 mg C/L and but sediment POC was consistently ≤1% by mass. Interestingly, the stream with the lowest and least bioavailable DOC concentration (1.2 mg C/L) also had the lowest sediment POC (reported as <0.5%), and demonstrated virtually no removal of DOC or DO in a 15-m long gravel bar (Sobczak & Findlay, 2002). However, when the same stream water was dosed into a hyporheic mesocosm containing different sediment, DO removal increased to approximately 33% while DOC concentrations actually rose by 9% (Figure 7 in Sobczak & Findlay, 2002). The percentage of POC in the new sediment was not reported, but substantial leaching of DOC in all mesocosm experiments suggested that the sediment used in their mesocosms had higher POC than any of the field sites (i.e., >1%). When water from two other streams with DOC of 3–5 mg C/L (and ≤1% POC) was dosed into these mesocosms with seemingly elevated sediment POC, the DO profiles that had been concave in the field became approximately linear along the mesocosm.

The importance of in situ carbon sources in the mesocosm can be quantified as a basis for the conceptual model in Figure 5. In our mesocosms, with the inflow of stream water set at 48 mL/min and an average DOC concentration

of 2 mg/L, stream water delivers approximately 50.4 g C as DOC to the inlet of the mesocosm each year. Given that POC constitutes 3% of the mass of the dry sediment in the mesocosms (with porosity of 40.4%), and assuming a density for the mineral solids of 2.57 g/cm^3 and density of the organic matter of 0.54 g/cm^3, then the 12-m long mesocosm has approximately 10 kg of organic carbon in storage (see Supplemental Info for calculation in Supporting Information S1). We know little about the relative bioavailability of these different organic carbon sources. Serchan et al. (2024) argued that stream-source DOC was likely to have limited bioavailability, especially in the summer, due to extremely high hyporheic turnover rates within the WS01 stream, resulting in extensive microbial processing of DOC when it reaches the watershed outlet. Yet some of the stored carbon must be reasonably bioavailable to support continued respiration in the mesocosm over 4 years with little change in underlying respiration rates.

Stream-sourced DOC does not appear to be a substantial energy source for hyporheic community respiration in the mesocosm, especially in the summer. Using a 1:1 respiratory quotient (calculated as the ratio of ΔDIC to ΔO_2), net changes in DOC from the inlet to the outlet of the 12-m mesocosm can only account for 5%–8% of respiration in the summer, based on DO consumption and DIC production, respectively. In the winter, the net change in DOC accounts for 12%–30% of the respiration. Of course, net changes may mask the actual utilization of stream-source DOC if respired DOC is replaced by DOC solubilized from in situ carbon along the 12-m flowpath. Dissolved organic carbon may also interact with sediment and POC through complex sorption-desorption processes across multiple spatiotemporal scales (e.g., Battin, 1999; Jardine et al., 1992; Zhou et al., 2019). Therefore, these carbon pools are not isolated and exist in a dynamic equilibrium that shapes carbon and nutrient cycling in aquatic ecosystems (Sobczak & Findlay, 2002; Wiegner et al., 2005). Because the DOC was not labeled in any way to differentiate its actual source, we cannot distinguish these processes. We can, however, compare gross inputs with loss of DO or production of DIC. In winter, if all influent DOC was respired, this could account for 45% of the DO consumed and 110% of the DIC produced. However, in the summer, influent DOC could only account for 27% and 41% of the respiration on a DO or DIC basis, respectively.

Overall, our finding that stream-sourced DOC had relatively little importance to the biogeochemistry of our mesocosms can be explained and integrated with other studies through the framework of Figure 5. In other words, studies may be placed on a continuum between end-member cases of low to high sediment:stream carbon ratios, matching the presence or absence, respectively, of initial hot spots across studies and sites. Our mesocosm study represents Figure 5b, with only 5%–30% respiration attributable to influent DOC (via net change). Serchan et al. found that DOC loss explained only 17% of DO consumption on average (range 0%–59% in individual sampling events). Another forested mountain catchment in the Danube basin reported 36% of summer DO consumption due to stream-derived DOC (Brugger, Wett, et al., 2001). In contrast, systems with predominantly stream-derived DOC versus sediment-derived organic carbon represent Figure 5a, promoting the formation of hot spots at the start of hyporheic flowpaths (e.g., Harvey et al., 2013) and linking overall hyporheic metabolism to influent carbon delivery. For example, Jones et al. (1995) found that limited in situ carbon (0.08% organic matter by mass even immediately after the deposition of fresh organic matter in a flood) only accounted for approximately 15% of hyporheic respiration compared to 85% from influent DOC. Under these conditions, nearly all the readily available stream-derived DOC would likely be exhausted in the initial portions of decameter-scale flowpaths. In our 12-m mesocosm, without substantial contributions of in situ carbon, distal portions of the flowpaths would have expressed lower reaction rates, which was not observed in this study.

We also note that in situ and influent carbon can vary in tandem in other systems. For example, layers of coarse benthic organic matter can reach >70% organic matter in streams with DOC concentrations of 3–4 mg C/L (Arango et al., 2007). Artificial woodchip bioreactors can represent high carbon end-members with nearly 100% organic matter and 40%–50% carbon in the sediments and stream DOC > 10 mg/L, yielding zeroth-order denitrification (e.g., Christianson et al., 2020; Hoover et al., 2016; Moorman et al., 2010; Robertson, 2010; Robertson & Merkley, 2009). The McMurdo Dry Valleys in Antarctica may represent a low carbon end-member, with DOC concentrations <0.6 mg C/L and sediment POC at 0.08% (e.g., Freckman & Virginia, 1997; Gooseff et al., 2002). A laboratory column experiment with artificial groundwater (without DO or DOC) upwelling through streambed sediments demonstrated that hotspots could occur at the end of flowpaths due to layers with higher POC (i.e., 3% vs. 0.2% by mass), highlighting the importance of heterogeneity and topology of in situ carbon layers (Gu et al., 2007). Synthesizing these studies demonstrates the importance of characterizing in situ versus influent reactant sources in different hyporheic systems, particularly when assessing biogeochemical reactions over the long spatial and temporal scales like those directly observed in the 12-m mesocosm (Figures 1

and 5). We recommend future studies focused on developing practical and cost-effective field methods for the characterization of in situ chemistry along decameter-scale flowpaths.

The relative proportion of in situ versus influent reactant sources also varied for DO, C, and N in the mesocosm, resulting in differential transport-versus reaction-limited conditions. Although we used zeroth-order rates in most of our analyses as they were the best-fit models, first-order rates also fit reasonably well and can be used to calculate the hyporheic Damköhler number ($Da_{HZ} = k$*transit time) as an illustrative example of balanced (i.e., $Da_{HZ} \sim 1$), transport-limited (i.e., $Da_{HZ} >> 1$), or reaction-limited (i.e., $Da_{HZ} << 1$) conditions (Harvey et al., 2013; Zarnetske et al., 2012). Oxygen came exclusively from influent stream water and had no in situ source, but removal was slow relative to transport times. In winter, the mesocosm was balanced for oxygen ($Da_{HZ, DO} = 1.19$). As described above, the faster consumption rate in summer led to more transport-limited conditions ($Da_{HZ,DO} = 4.25$). Carbon had a predominantly in situ source that was not consumed quickly, leading to reaction-limited conditions throughout the flowpath. Because the DOC consumption and DIC production slowed under anoxic conditions, the flowpath became more reaction-limited in summer ($Da_{HZ,DOC} = 0.19$; $Da_{HZ,DIC} = 0.23$) than in winter ($Da_{HZ,DOC} = 0.35$; $Da_{HZ,DIC} = 0.32$). Nitrogen had intermediate behavior between oxygen and carbon, as there was an in situ source that was approximately equal to influent sources. This caused reaction-limited conditions for TDN during oxic portions ($Da_{HZ, TDN} = 0.40$ in winter, 0.42 for first 7-m in summer). With anoxia, denitrification occurred rapidly, leading to balanced conditions in the overall mesocosm ($Da_{HZ, DENIT} = 1.02$) and slightly transport-limited conditions in the last 5 m ($Da_{HZ, DENIT} = 1.76$).

The differences between constituents and seasons highlight the variability of mass transfer characterization in hyporheic flowpaths and suggest solute-specific complexities that cannot be easily predicted from transit times alone. In WS01, a steep, gravel-bedded mountainous stream, hyporheic flow is primarily driven by gravitational head gradients generated by the longitudinal profile of the stream (Wondzell et al., 2022). These gradients are static and thus, porewater velocity and transit time should change little between seasons. Lower gradient sand-bedded streams may function quite differently. In these streams, surface flow velocity interacting with channel bedforms creates pressure gradients that drive hyporheic exchange (Wondzell et al., 2022). Discharge and flow velocity change seasonally and with storms in these streams. The resulting changes in pressure gradients should lead to systematic changes in porewater velocity through the hyporheic zone and these changes have the potential to change the underlying biogeochemistry. For example, faster porewater velocities (i.e., shorter transit times) are expected to lead to more reaction-limited conditions, extension of bulk oxic conditions, and higher export of nitrate (e.g., Gu et al., 2007; Hampton et al., 2020; Kaufman et al., 2017; Pusch, 1996; Sobczak & Findlay, 2002). However, velocity can also impact reaction rates in non-linear or even inconsistent patterns. Hampton et al. (2020) found the highest rates for DO and nitrate attenuation at a velocity of 0.8 m/d, lowest at 2 m/d, and intermediate at 3 m/d. Further, DOC decreased along flowpaths at the highest velocity, but accumulated along the same flowpaths at lower velocities (Hampton et al., 2020). Dissolved organic carbon and in situ carbon are not independent pools (Gu et al., 2007; Pusch, 1996; Sobczak & Findlay, 2002), and velocity changes can drive complicated interactions with redox zonation, accumulation versus mobilization of DOC, and flow-dependent exchange rates between bulk porewater and less mobile zones (Briggs et al., 2018) around POC and biofilms. Finally, velocity is not typically altered in isolation, but rather alongside numerous seasonal changes such as stream discharge, DOC and in situ carbon loading and bioavailability, groundwater upwelling and mixing, flowpath geometry shifts, and changes in sediment permeability in response to deposition and scour dynamics. For example, Dorley et al. (2022) found complex interactions between hydrology, resource supply, and biological function when determining drivers of in-stream respiration in a headwater stream subject to multiple rounds of stoichiometric treatments and flow conditions. Future work should consider these manifold factors in mediating biogeochemistry along decameter-scale flowpaths in field settings.

4.3. Particulate and Sediment-Bound Organic Carbon Could Support Respiration in Decameter-Scale Flowpaths Over Several Centuries

Dissolved organic carbon can be sorbed, consumed, transformed, and generated within the mesocosms so that net changes in concentrations from the mesocosm inlets to the outlets do not necessarily represent the utilization of stream-derived DOC (Serchan et al., 2024; Sobczak & Findlay, 2002). However, several factors suggest that stream-derived DOC was not the principal substrate for hyporheic metabolism. First, DIC generation exceeded apparent DOC consumption by 84 mg/day in winter and 136 mg/day in summer. Similar results for in situ DOC utilization and DIC production have also been measured in the WS01 well network (Corson-Rikert et al., 2016)

and 6 replicates of our same mesocosm in 2-m flowpath configurations (Serchan et al., 2024). Further, a 10-year carbon budget for WS01 found that DIC accounted for 40.4% of total carbon exports, compared to 22.0% as POC and only 11.2% as DOC (Argerich et al., 2016). As discussed by Serchan et al. (2024), other explanations for excess DIC generation could include weathering of carbonate minerals or chemolithotrophic processes, but are unlikely given the predominately siliceous rock in WS01 and oxic-to-weakly-reducing conditions in the mesocosm, respectively. Seasonal sorption-desorption or assimilation and release by biofilms are also unlikely, as DIC generation has exceeded DOC consumption on all sample dates in the WS01 well field, 2-m mesocosm, and 12-m mesocosm (Corson-Rikert et al., 2016; Serchan et al., 2024). Each month of the year was represented at least once in the sampling dates across an approximately 6-year period of observation. Second, Serchan et al. found linear changes in DO, DOC, and DIC with travel time through the mesocosm that were best fit by zeroth-order kinetics. If readily bioavailable stream-derived DOC was the principal substrate for metabolism, they should have seen much higher metabolism rates in the first meter of their mesocosm than in the second. Our results, using the same mesocosm facility but configured into a 12-m long flow path, demonstrated that the zeroth-order kinetics were persistent for flowpaths with up to 54-hr transit times as long as the bulk hyporheic water did not go anoxic. While Serchan et al. hypothesized that in situ carbon sources continued to facilitate DOC-dependent reactions through their 2-m mesocosms, our observation of sustained DOC-dependent reactions over 12-m long, 54-hr flowpaths conclusively demonstrates in situ DOC generation, likely from sources such as POC, microbial decomposition, and OC desorption. Serchan et al. also found consistent decreases in the respiratory quotient with time since initially packing the mesocosms (from 2016 through 2018), a pattern that could only be related to changes in the bioavailability of POC over time. Finally, our results showing increases in TDN along the oxic portions of the 12-m mesocosm further emphasize the importance of particulate organics in hyporheic metabolism because the increases in TDN were consistent with the decomposition of organic substrate.

Thus, the present experiment strongly supports the conclusion that aerobic respiration of POC is the primary biogeochemical process occurring in the 12-m mesocosm, followed by denitrification using POC in the anoxic portions of the flowpath in summer. The potential for POC to be the primary fuel for heterotrophic metabolism in hyporheic zones is not novel in theory, but has been understudied (Serchan et al., 2024) and underestimated because few, if any, studies have quantitatively compared the roles of DOC versus POC in hyporheic zones with very low concentrations of DOC and high concentrations of POC. The primary role of POC is particularly relevant to decameter-scale flowpaths, as in situ carbon sources can sustain heterotrophic metabolism over long spatial scales if the lifespan of the POC is also adequate to sustain metabolism over long time periods. Building on the prior work of WS01 hyporheic mesocosm research, we see evidence of k_{DIC} converging toward a stable long-term reaction rate. Serchan et al. calculated both k_{O2} (for oxygen consumption) and k_{DIC} (for DIC generation) in their 2-m mesocosms and compared these against time since packing the mesocosms with streambed sediment. They observed a strong decrease in metabolic rates (based on k_{DIC}) and speculated that the lack of a relationship based on k_{O2} resulted from changes in the quality and molecular composition of POC with time, which was reflected in a significant decreasing trend in the respiratory quotient over this same period (Serchan et al., 2024). Our samples were collected approximately 1.5–2 years after the last measurements taken by Serchan et al., but the rates we observed for k_{O2}, k_{DIC}, and k_{DOC} fell within the ranges of their earlier measurements. Thus, our results suggest that the readily available in situ carbon that created high metabolic rates in the first years after packing the mesocosms has been consumed, causing metabolic rates to stabilize. While the metabolic rates we observed in the 12-m mesocosm remained higher than those observed in the nearby WS01 hyporheic well network (Serchan et al., 2024), the fact that they have stabilized suggests that the hyporheic zone can maintain the current metabolic activity for a considerable time.

The lifespan of in situ carbon stocks can be estimated by dividing the mass of organic carbon by the consumption rate (Findlay & Sobczak, 1996; Gu et al., 2007; Pusch, 1996). Previous studies with relatively rapid carbon consumption rates in flowpaths of ≤0.5 m length estimated that in situ carbon would be fully consumed at timescales of months to years, but also hypothesized that reburial of POC at sub-annual timescales would provide an effectively continuous supply of in situ carbon (Gu et al., 2007; Pusch, 1996). We calculated the approximate lifespan for in situ carbon stocks in the 12-m mesocosm based on the average net DIC flux observed in this study and reasonable assumptions for the density of the 3% in situ carbon by mass composed of wood fragments. In such conditions, the quantity of in situ carbon in the mesocosm is expected to fuel hyporheic metabolism for approximately 250 years or more (Text S1 in Supporting Information S1). This timescale calculation is dependent on numerous assumptions, most notably an extrapolation of observed DIC production rates into the distant future.

However, it provides an illustrative example of the potential long-term relevance of decameter-scale flowpaths. Even with different sets of assumptions (Text S1 in Supporting Information S1), the range of estimated carbon lifespans in the mesocosm overlaps with the range of geometric means for the carbon turnover time of coarse woody debris in aquatic environments of up to 250 years (Table 3 in Hedin, 1990) and aligns with observations of large wood that is over 450 years old in HJA streams (Table 11 in Harmon et al., 1986). Further, this carbon utilization timescale loosely aligns with the return intervals between debris avalanches and torrents that reset valley floors and the sediment (including new burial of large wood as POC) they contain at intervals on the order of several centuries, although these return intervals have estimated uncertainty of +60% to −100% (Swanson et al., 1982). Thus, relatively slow rates of carbon utilization, combined with periodic recharge of buried carbon, could support sustained metabolism along decameter-scale flowpaths as a continuous hyporheic function.

5. Conclusions

1. Hyporheic biogeochemistry for DO, N, and C changed significantly between summer and winter in the 12-m mesocosm. Hyporheic flow was fully oxic and a net nitrogen source in both summer and winter in the first 6m of the mesocosm. In contrast, the full 12 m flowpath was variably oxic/anoxic and a net source/sink for nitrogen depending on seasonal fluctuations in hyporheic temperature.
2. We did not observe any hot spots in the mesocosm. Instead, most reactions were zeroth-order over 12 m and 54 hr of transit time (excepting DO and nitrate following the transition to anoxic conditions in summer).
3. Influent chemistry had much less impact on hyporheic biogeochemistry than expected because of a high ratio of in situ reactant sources compared to stream-derived reactant sources. Specifically, sorbed DOC or buried POC likely fueled transformations of DO and N, with DIC and TIN production rates based on temperature and redox conditions. Slow DOC consumption rates suggest that large stores of in situ carbon can fuel hyporheic metabolism for hundreds of years.
4. Each reactant in our study had a different hyporheic Damköhler number due to differences in reaction rates, redox sensitivity, and in situ versus stream-derived sources. These solute-specific findings highlight the challenge of characterizing a flowpath as reaction- or transport-limited even when geometry and transit time are held constant.
5. This mesocosm study provides a unique data set to inspire and be used by future modeling studies seeking to investigate decameter-scale flowpaths in relatively nutrient limited streams typical of many headwater streams in temperate and Mediterranean regions. Continued research should focus on testing for the presence and biogeochemical contributions of decameter-scale flowpaths in the field, especially in watersheds with different amounts of influent and in situ reactant sources.

Data Availability Statement

Archiving is underway for all water quality data used in this study. Data files are in the process of submission to the H.J. Andrews Experimental Forest data repository and can be accessed at https://doi.org/10.6073/pasta/b31d4b2748e4eb1d67136d81f1e3227e.

Acknowledgments
Construction of the hyporheic mesocosm facility was funded by the National Science Foundation under the grant EAR-1417603, with additional funding contributed by the United States Forest Service, Pacific Northwest Research Station, with continued support for the facility through the H. J. Andrews Experimental Forest. Oregon State University's College of Earth, Ocean, and Atmospheric Sciences machinist, Ben Russell, helped design and then build the mesocosms. SPH and ASW were supported by NSF Award EAR-1652293. RGP was funded through NSF HDR-1914490. Background climate, stream flow, and biogeochemistry data along with other site facilities were provided by the H. J. Andrews Experimental Forest and Long Term Ecological Research (LTER) program, administered cooperatively by Oregon State University, the USDA Forest Service Pacific Northwest Research Station, and the Willamette National Forest and supported by the National Science Foundation under the Grants DEB-1440409 and DEB-2025755. We thank the H.J. Andrews Experimental Forest staff for their support with project logistics over several years. We also thank the H.J. Andrews community, who supported this project team personally and professionally through challenging times, including several wildfires and the Covid-19 pandemic. We thank many graduate and undergraduate students for their assistance with mesocosm maintenance and sampling. We also thank Dr. Roy Haggerty for assistance with calculations for the projected lifespan of in situ carbon in the mesocosm.

References

Arango, C. P., Tank, J. L., Schaller, J. L., Royer, T. V., Bernot, M. J., & David, M. B. (2007). Benthic organic carbon influences denitrification in streams with high nitrate concentration. *Freshwater Biology*, *52*(7), 1210–1222. https://doi.org/10.1111/j.1365-2427.2007.01758.x

Argerich, A., Haggerty, R., Johnson, S. L., Wondzell, S. M., Dosch, N., Corson-Rikert, H., et al. (2016). Comprehensive multiyear carbon budget of a temperate headwater stream. *Journal of Geophysical Research: Biogeosciences*, *121*(5), 1306–1315. https://doi.org/10.1002/2015JG003050

Argerich, A., Martí, E., Sabater, F., & Ribot, M. (2011). Temporal variation of hydrological exchange and hyporheic biogeochemistry in a headwater stream during autumn. *Journal of the North American Benthological Society*, *30*(3), 635–652. https://doi.org/10.1899/10-078.1

Arnon, S., Gray, K. A., & Packman, A. I. (2007). Biophysicochemical process coupling controls nitrogen use by benthic biofilms. *Limnology & Oceanography*, *52*(4), 1665–1671. https://doi.org/10.4319/lo.2007.52.4.1665

Battin, T. J. (1999). Hydrologic flow paths control dissolved organic carbon fluxes and metabolism in an alpine stream hyporheic zone. *Water Resources Research*, *35*(10), 3159–3169. https://doi.org/10.1029/1999WR900144

Battin, T. J., Kaplan, L. A., Denis Newbold, J., & Hansen, C. M. E. (2003). Contributions of microbial biofilms to ecosystem processes in stream mesocosms. *Nature*, *426*(6965), 439–442. https://doi.org/10.1038/nature02152

Blöschl, G., & Sivapalan, M. (1995). Scale issues in hydrological modelling: A review. *Hydrological Processes*, *9*(3-4), 251–290. https://doi.org/10.1002/hyp.3360090305

Boano, F., Harvey, J. W., Marion, A., Packman, A. I., Revelli, R., Ridolfi, L., & Wörman, A. (2014). Hyporheic flow and transport processes: Mechanisms, models, and biogeochemical implications. *Reviews of Geophysics*, *52*(4), 603–679. https://doi.org/10.1002/2012RG000417

Briggs, M. A., Day-Lewis, F. D., Dehkordy, F. M. P., Hampton, T., Zarnetske, J. P., Scruggs, C. R., et al. (2018). Direct observations of hydrologic exchange occurring with less-mobile porosity and the development of anoxic microzones in sandy lakebed sediments. *Water Resources Research*, *54*(7), 4714–4729. https://doi.org/10.1029/2018WR022823

Brugger, A., Reitner, B., Kolar, I., Quéric, N., & Herndl, G. J. (2001). Seasonal and spatial distribution of dissolved and particulate organic carbon and bacteria in the bank of an impounding reservoir on the Enns River, Austria. *Freshwater Biology*, *46*(8), 997–1016. https://doi.org/10.1046/j.1365-2427.2001.00743.x

Brugger, A., Wett, B., Kolar, I., Reitner, B., & Herndl, G. J. (2001). Immobilization and bacterial utilization of dissolved organic carbon entering the riparian zone of the alpine Enns River, Austria. *Aquatic Microbial Ecology*, *24*(2), 129–142. https://doi.org/10.3354/ame024129

Buffington, J. M., & Tonina, D. (2009). Hyporheic exchange in mountain rivers II: Effects of channel morphology on mechanics, scales, and rates of exchange. *Geography Compass*, *3*(3), 1038–1062. https://doi.org/10.1111/j.1749-8198.2009.00225.x

Christianson, L. E., Feyereisen, G. W., Hay, C., Tschirner, U. W., Kult, K., Wickramarathne, N. M., & Soupir, M. L. (2020). Denitrifying bioreactor woodchip recharge: Media properties after nine years. *Transactions of the ASABE*, *63*(2), 407–416. https://doi.org/10.13031/trans.13709

Corson-Rikert, H. A., Wondzell, S. M., Haggerty, R., & Santelmann, M. V. (2016). Carbon dynamics in the hyporheic zone of a headwater mountain stream in the Cascade Mountains, Oregon. *Water Resources Research*, *52*(10), 7556–7576. https://doi.org/10.1002/2016WR019303

Dorley, J., Singley, J., Covino, T., Singha, K., Gooseff, M., González-Pinzón, R., & González-Pinzón, R. (2022). Physical and stoichiometric controls on stream respiration in a headwater stream. *Biogeosciences Discussions*, *2022*(15), 1–22. https://doi.org/10.5194/bg-20-3353-2023

Findlay, S., & Sobczak, W. V. (1996). Variability in removal of dissolved organic carbon in hyporheic sediments. *Journal of the North American Benthological Society*, *15*(1), 35–41. https://doi.org/10.2307/1467431

Findlay, S., Strayer, D., Goumbala, C., & Gould, K. (1993). Metabolism of streamwater dissolved organic carbon in the shallow hyporheic zone. *Limnology & Oceanography*, *38*(7), 1493–1499. https://doi.org/10.4319/lo.1993.38.7.1493

Findlay, S. E., & Arsuffi, T. L. (1989). Microbial growth and detritus transformations during decomposition of leaf litter in a stream. *Freshwater Biology*, *21*(2), 261–269. https://doi.org/10.1111/j.1365-2427.1989.tb01364.x

Freckman, D. W., & Virginia, R. A. (1997). Low-diversity Antarctic soil nematode communities: Distribution and response to disturbance. *Ecology*, *78*(2), 363–369. https://doi.org/10.1890/0012-9658(1997)078[0363:LDASNC]2.0.CO;2

Fritz, K. M., Feminella, J. W., Colson, C., Lockaby, B. G., Governo, R., & Rummer, R. B. (2006). Biomass and decay rates of roots and detritus in sediments of intermittent coastal plain streams. *Hydrobiologia*, *556*(1), 265–277. https://doi.org/10.1007/s10750-005-1154-9

Gooseff, M. N., McKnight, D. M., Lyons, W. B., & Blum, A. E. (2002). Weathering reactions and hyporheic exchange controls on stream water chemistry in a glacial meltwater stream in the McMurdo Dry Valleys. *Water Resources Research*, *38*(12), 15–1–15–17. https://doi.org/10.1029/2001WR000834

Gooseff, M. N., McKnight, D. M., Runkel, R. L., & Vaughn, B. H. (2003). Determining long time-scale hyporheic zone flow paths in Antarctic streams. *Hydrological Processes*, *17*(9), 1691–1710. https://doi.org/10.1002/hyp.1210

Gregory, S., & Johnson, S. (2019). *Stream and air temperature data from stream gages and stream confluences in the Andrews Experimental Forest, 1950 to present. Long-Term Ecological Research*. Forest Science Data Bank. [Database]. Retrieved from http://andlter.forestry.oregonstate.edu/data/abstract.aspx?dbcode=HT004

Gu, C., Hornberger, G. M., Mills, A. L., Herman, J. S., & Flewelling, S. A. (2007). Nitrate reduction in streambed sediments: Effects of flow and biogeochemical kinetics. *Water Resources Research*, *43*(12). https://doi.org/10.1029/2007WR006027

Hampton, T. B., Zarnetske, J. P., Briggs, M. A., MahmoodPoor Dehkordy, F., Singha, K., Day-Lewis, F. D., et al. (2020). Experimental shifts of hydrologic residence time in a sandy urban stream sediment–water interface alter nitrate removal and nitrous oxide fluxes. *Biogeochemistry*, *149*(2), 195–219. https://doi.org/10.1007/s10533-020-00674-7

Hampton, T. B., Zarnetske, J. P., Briggs, M. A., Singha, K., Harvey, J. W., Day-Lewis, F. D., et al. (2019). Residence time controls on the fate of nitrogen in flow-through lakebed sediments. *Journal of Geophysical Research: Biogeosciences*, *124*(3), 689–707. https://doi.org/10.1029/2018JG004741

Harmon, M. E., Franklin, J. F., Swanson, F. J., Sollins, P., Gregory, S., Lattin, J., et al. (1986). Ecology of coarse woody debris in temperate ecosystems. *Advances in Ecological Research*, *15*, 133–302. https://doi.org/10.1016/S0065-2504(08)60121-X

Harvey, B. N., Johnson, M. L., Kiernan, J. D., & Green, P. G. (2011). Net dissolved inorganic nitrogen production in hyporheic mesocosms with contrasting sediment size distributions. *Hydrobiologia*, *658*(1), 343–352. https://doi.org/10.1007/s10750-010-0504-4

Harvey, J. W., Böhlke, J. K., Voytek, M. A., Scott, D., & Tobias, C. R. (2013). Hyporheic zone denitrification: Controls on effective reaction depth and contribution to whole-stream mass balance. *Water Resources Research*, *49*(10), 6298–6316. https://doi.org/10.1002/wrcr.20492

Harvey, J. W., & Wagner, B. J. (2000). Quantifying hydrologic interactions between streams and their subsurface hyporheic zones. *Streams and Ground Waters*, 3–44. https://doi.org/10.1016/b978-012389845-6/50002-8

Hedin, L. O. (1990). Factors controlling sediment community respiration in Woodland stream ecosystems. *Oikos*, *57*(1), 94–105. https://doi.org/10.2307/3565742

Herzog, S. P., Galloway, J., Banks, E. W., Posselt, M., Jaeger, A., Portmann, A., et al. (2023). Combined surface-subsurface stream restoration structures can optimize hyporheic attenuation of stream water contaminants. *Environmental Science and Technology*, *57*(10), 4153–4166. https://doi.org/10.1021/acs.est.2c05967

Herzog, S. P., Ward, A. S., & Wondzell, S. M. (2019). Multiscale feature-feature interactions control patterns of hyporheic exchange in a simulated headwater mountain stream. *Water Resources Research*, *55*(12), 10976–10992. https://doi.org/10.1029/2019WR025763

Hester, E. T., Cardenas, M. B., Haggerty, R., & Apte, S. V. (2017). The importance and challenge of hyporheic mixing. *Water Resources Research*, *53*(5), 3565–3575. https://doi.org/10.1002/2016WR020005

Hoover, N. L., Bhandari, A., Soupir, M. L., & Moorman, T. B. (2016). Woodchip denitrification bioreactors: Impact of temperature and hydraulic retention time on nitrate removal. *Journal of Environmental Quality*, *45*(3), 803–812. https://doi.org/10.2134/jeq2015.03.0161

Inwood, S. E., Tank, J. L., & Bernot, M. J. (2005). Patterns of denitrification associated with land use in 9 midwestern headwater streams. *Journal of the North American Benthological Society*, *24*(2), 227–245. https://doi.org/10.1899/04-032.1

Jardine, P. M., Dunnivant, F. M., Selim, H. M., & McCarthy, J. F. (1992). Comparison of models for describing the transport of dissolved organic carbon in aquifer columns. *Soil Science Society of America Journal*, *56*(2), 393–401. https://doi.org/10.2136/sssaj1992.03615995005600020009x

Johnson, S., & Fredriksen, R. (2019). *Stream chemistry concentrations and fluxes using proportional sampling in the Andrews Experimental Forest, 1968 to present. Long-Term Ecological Research*. Forest Science Data Bank. [Database]. Retrieved from http://andlter.forestry.oregonstate.edu/data/abstract.aspx?dbcode=CF002

Johnson, S., Henshaw, D., Downing, G., Wondzell, S., Schulze, M., Kennedy, A., et al. (2021). Long-term hydrology and aquatic biogeochemistry data from H. J. Andrews experimental forest, cascade mountains, Oregon. *Hydrological Processes*, *35*(5), e14187. https://doi.org/10.1002/hyp.14187

Johnson, S., Wondzell, S., & Rothacher, J. (2024). *Stream discharge in gaged watersheds at the HJ Andrews Experimental Forest, 1949 to present*. Long-Term Ecological Research. Forest Science Data Bank. [Database]. Retrieved from http://andlter.forestry.oregonstate.edu/data/abstract.aspx?dbcode=HF004

Jones, J. B., Fisher, S. G., & Grimm, N. B. (1995). Nitrification in the hyporheic zone of a desert stream ecosystem. *Journal of the North American Benthological Society*, *14*(2), 249–258. https://doi.org/10.2307/1467777

Kaufman, M. H., Cardenas, M. B., Buttles, J., Kessler, A. J., & Cook, P. L. (2017). Hyporheic hot moments: Dissolved oxygen dynamics in the hyporheic zone in response to surface flow perturbations. *Water Resources Research*, *53*(8), 6642–6662. https://doi.org/10.1002/2016WR020296

Knapp, J. L. A., González-Pinzón, R., Drummond, J. D., Larsen, L. G., Cirpka, O. A., & Harvey, J. W. (2017). Tracer-based characterization of hyporheic exchange and benthic biolayers in streams. *Water Resources Research*, *53*(2), 1575–1594. https://doi.org/10.1002/2016WR019393

Krause, S., Lewandowski, J., Grimm, N. B., Hannah, D. M., Pinay, G., McDonald, K., et al. (2017). Ecohydrological interfaces as hot spots of ecosystem processes. *Water Resources Research*, *53*(8), 6359–6376. https://doi.org/10.1002/2016WR019516

Lewandowski, J., Putschew, A., Schwesig, D., Neumann, C., & Radke, M. (2011). Fate of organic micropollutants in the hyporheic zone of a eutrophic lowland stream: Results of a preliminary field study. *Science of the Total Environment*, *409*(10), 1824–1835. https://doi.org/10.1016/j.scitotenv.2011.01.028

Liu, Y., Liu, C., Nelson, W. C., Shi, L., Xu, F., Liu, Y., et al. (2017). Effect of water chemistry and hydrodynamics on nitrogen transformation activity and microbial community functional potential in hyporheic zone sediment columns. *Environmental Science and Technology*, *51*(9), 4877–4886. https://doi.org/10.1021/acs.est.6b05018

Lowell, J. L., Gordon, N., Engstrom, D., Stanford, J. A., Holben, W. E., & Gannon, J. E. (2009). Habitat heterogeneity and associated microbial community structure in a small-scale floodplain hyporheic flow path. *Microbial Ecology*, *58*(3), 611–620. https://doi.org/10.1007/s00248-009-9525-9

Marzadri, A., Tonina, D., & Bellin, A. (2013). Quantifying the importance of daily stream water temperature fluctuations on the hyporheic thermal regime: Implication for dissolved oxygen dynamics. *Journal of Hydrology*, *507*, 241–248. https://doi.org/10.1016/j.jhydrol.2013.10.030

McClain, M. E., Boyer, E. W., Dent, C. L., Gergel, S. E., Grimm, N. B., Groffman, P. M., et al. (2003). Biogeochemical hot spots and hot moments at the interface of terrestrial and aquatic ecosystems. *Ecosystems*, *6*(4), 301–312. https://doi.org/10.1007/s10021-003-0161-9

Mermillod-Blondin, F., Gaudet, J.-P., Gérino, M., Desrosiers, G., & Creuzé des Châtelliers, M. (2003). Influence of macroinvertebrates on physico-chemical and microbial processes in hyporheic sediments. *Hydrological Processes*, *17*(4), 779–794. https://doi.org/10.1002/hyp.1165

Moorman, T. B., Parkin, T. B., Kaspar, T. C., & Jaynes, D. B. (2010). Denitrification activity, wood loss, and N2O emissions over 9 years from a wood chip bioreactor. *Ecological Engineering*, *36*(11), 1567–1574. https://doi.org/10.1016/j.ecoleng.2010.03.012

Navel, S., Mermillod-Blondin, F., Montuelle, B., Chauvet, E., Simon, L., & Marmonier, P. (2011). Water–sediment exchanges control microbial processes associated with leaf litter degradation in the hyporheic zone: A microcosm study. *Microbial Ecology*, *61*(4), 968–979. https://doi.org/10.1007/s00248-010-9774-7

Nelson, W. C., Graham, E. B., Crump, A. R., Fansler, S. J., Arntzen, E. V., Kennedy, D. W., & Stegen, J. C. (2020). Distinct temporal diversity profiles for nitrogen cycling genes in a hyporheic microbiome. *PLoS One*, *15*(1), e0228165. https://doi.org/10.1371/journal.pone.0228165

Nogueira, G. E. H., Schmidt, C., Brunner, P., Graeber, D., & Fleckenstein, J. H. (2021). Transit-time and temperature control the spatial patterns of aerobic respiration and denitrification in the riparian zone. *Water Resources Research*, *57*(12), e2021WR030117. https://doi.org/10.1029/2021WR030117

Payn, R. A., Gooseff, M. N., McGlynn, B. L., Bencala, K. E., & Wondzell, S. M. (2009). Channel water balance and exchange with subsurface flow along a mountain headwater stream in Montana, United States. *Water Resources Research*, *45*(11). https://doi.org/10.1029/2008WR007644

Peter, K. T., Herzog, S., Tian, Z., Wu, C., McCray, J. E. J. E., Lynch, K., & Kolodziej, E. P. E. P. (2019). Evaluating emerging organic contaminant removal in an engineered hyporheic zone using high resolution mass spectrometry. *Water Research*, *150*, 140–152. https://doi.org/10.1016/J.WATRES.2018.11.050

Peterson, E. W., & Sickbert, T. B. (2006). Stream water bypass through a meander neck, laterally extending the hyporheic zone. *Hydrogeology Journal*, *14*(8), 1443–1451. https://doi.org/10.1007/s10040-006-0050-3

Pusch, M. (1996). The metabolism of organic matter in the hyporheic zone of a mountain stream, and its spatial distribution. *Hydrobiologia*, *323*(2), 107–118. https://doi.org/10.1007/BF00017588

Quick, A. M., Reeder, W. J., Farrell, T. B., Tonina, D., Feris, K. P., & Benner, S. G. (2016). Controls on nitrous oxide emissions from the hyporheic zones of streams. *Environmental Science and Technology*, *50*(21), 11491–11500. https://doi.org/10.1021/acs.est.6b02680

Robertson, W. D. (2010). Nitrate removal rates in woodchip media of varying age. *Ecological Engineering*, *36*(11), 1581–1587. https://doi.org/10.1016/j.ecoleng.2010.01.008

Robertson, W. D., & Merkley, L. C. (2009). In-stream bioreactor for agricultural nitrate treatment. *Journal of Environmental Quality*, *38*(1), 230–237. https://doi.org/10.2134/jeq2008.0100

Roy Chowdhury, S., Zarnetske, J. P., Phanikumar, M. S., Briggs, M. A., Day-Lewis, F. D., & Singha, K. (2020). Formation criteria for hyporheic anoxic microzones: Assessing interactions of hydraulics, nutrients, and biofilms. *Water Resources Research*, *56*(3), 1–15. https://doi.org/10.1029/2019WR025971

Rutere, C., Posselt, M., & Horn, M. A. (2020). Fate of trace organic compounds in hyporheic zone sediments of contrasting organic carbon content and impact on the microbiome. *Water*, *12*(12), 3518. https://doi.org/10.3390/w12123518

Sawyer, A. H. (2015). Enhanced removal of groundwater-borne nitrate in heterogeneous aquatic sediments. *Geophysical Research Letters*, *42*(2), 403–410. https://doi.org/10.1002/2014GL062234

Schmadel, N. M., Ward, A. S., & Wondzell, S. M. (2017). Hydrologic controls on hyporheic exchange in a headwater mountain stream. *Water Resources Research*, *53*(7), 6260–6278. https://doi.org/10.1002/2017WR020576

Serchan, S. P. (2021). *Evidence of buried particulate organic carbon as foundation for heterotrophic carbon metabolism in the hyporheic zone of a montane headwater stream in the H. J.* Andrews Experimental Forest.

Serchan, S. P., Wondzell, S. M., Haggerty, R., Pennington, R., Feris, K., Sanfilippo, A., et al. (2024). Buried particulate organic carbon fuels heterotrophic metabolism in the hyporheic zone of a montane headwater stream. *Freshwater Science*, *43*(3), 288–306. https://doi.org/10.1086/731772

Sheibley, R. W., Jackman, A. P., Duff, J. H., & Triska, F. J. (2003). Numerical modeling of coupled nitrification–denitrification in sediment perfusion cores from the hyporheic zone of the Shingobee River, MN. *Advances in Water Resources*, *26*(9), 977–987. https://doi.org/10.1016/S0309-1708(03)00088-5

Siegrist, R. L. (2016). Decentralized water reclamation engineering: A curriculum workbook. *Decentralized Water Reclamation Engineering: A Curriculum Workbook*. https://doi.org/10.1007/978-3-319-40472-1

Sobczak, W. V., & Findlay, S. (2002). Variation in bioavailability of dissolved organic carbon among stream hyporheic flowpaths. *Ecology*, *83*(11), 3194–3209. https://doi.org/10.1890/0012-9658(2002)083[3194:VIBODO]2.0.CO;2

Sobczak, W. V., Findlay, S., & Dye, S. (2003). Relationships between DOC bioavailability and nitrate removal in an upland stream: An experimental approach. *Biogeochemistry*, *62*(3), 309–327. https://doi.org/10.1023/A:1021192631423

Sobczak, W. V., Hedin, L. O., & Klug, M. J. (1998). Relationships between bacterial productivity and organic carbon at a soil—Stream interface. *Hydrobiologia*, *386*(1/3), 45–53. https://doi.org/10.1023/A:1003583813445

Swanson, F. J., Fredriksen, R., & McCorison, F. (1982). Material transfer in a western Oregon forested watershed.

Tóth, J. (1963). A theoretical analysis of groundwater flow in small drainage basins. *Journal of Geophysical Research*, *68*(16), 4795–4812. https://doi.org/10.1029/JZ068i016p04795

Trauth, N., Schmidt, C., Vieweg, M., Maier, U., & Fleckenstein, J. H. (2014). Hyporheic transport and biogeochemical reactions in pool-riffle systems under varying ambient groundwater flow conditions. *Journal of Geophysical Research: Biogeosciences*, *119*(5), 910–928. https://doi.org/10.1002/2013JG002586

Valett, H. M., Fisher, S. G., & Stanley, E. H. (1990). Physical and chemical characteristics of the hyporheic zone of a Sonoran Desert stream. *Journal of the North American Benthological Society*, *9*(3), 201–215. https://doi.org/10.2307/1467584

Ward, A. S. (2016). The evolution and state of interdisciplinary hyporheic research. *Wiley Interdisciplinary Reviews: Water*, *3*(1), 83–103. https://doi.org/10.1002/wat2.1120

Ward, A. S., Gooseff, M. N., Voltz, T. J., Fitzgerald, M., Singha, K., & Zarnetske, J. P. (2013). How does rapidly changing discharge during storm events affect transient storage and channel water balance in a headwater mountain stream? *Water Resources Research*, *49*(9), 5473–5486. https://doi.org/10.1002/wrcr.20434

Ward, A. S., & Packman, A. I. (2019). Advancing our predictive understanding of river corridor exchange. *Wiley Interdisciplinary Reviews: Water*, *6*(1), e1327. https://doi.org/10.1002/wat2.1327

Ward, A. S., Schmadel, N. M., & Wondzell, S. M. (2018a). Simulation of dynamic expansion, contraction, and connectivity in a mountain stream network. *Advances in Water Resources*, *114*, 64–82. https://doi.org/10.1016/J.ADVWATRES.2018.01.018

Ward, A. S., Schmadel, N. M., & Wondzell, S. M. (2018b). Time-variable transit time distributions in the hyporheic zone of a headwater mountain stream. *Water Resources Research*, *54*(3), 2017–2036. https://doi.org/10.1002/2017WR021502

Ward, A. S., Wondzell, S. M., Gooseff, M. N., Covino, T., Herzog, S., McGlynn, B., & Payn, R. A. (2023). Breaking the window of detection: Using multi-scale solute tracer studies to assess mass recovery at the detection limit. *Water Resources Research*, *59*(3), e2022WR032736. https://doi.org/10.1029/2022wr032736

Ward, A. S., Wondzell, S. M., Schmadel, N. M., & Herzog, S. P. (2020). Climate change causes river network contraction and disconnection in the HJ Andrews Experimental Forest, Oregon, USA. *Frontiers in Water*, *2*, 7. https://doi.org/10.3389/frwa.2020.00007

Wiegner, T. N., Kaplan, L. A., Newbold, J. D., & Ostrom, P. H. (2005). Contribution of dissolved organic C to stream metabolism: A mesocosm study using 13C-enriched tree-tissue leachate. *Journal of the North American Benthological Society*, *24*(1), 48–67. https://doi.org/10.1899/0887-3593(2005)024<0048:CODOCT>2.0.CO;2

Wondzell, S. M., Herzog, S. P., Gooseff, M. N., Ward, A. S., & Schmadel, N. M. (2022). 6.22 - Geomorphic controls on hyporheic exchange across scales—Watersheds to particles. In J. Jack & F. Shroder (Eds.), *Treatise on geomorphology* (2nd ed., pp. 409–429). Academic Press. https://doi.org/10.1016/B978-0-12-409548-9.12135-9

Zarnetske, J. P., Gooseff, M. N., Bowden, W. B., Greenwald, M. J., Brosten, T. R., Bradford, J. H., & McNamara, J. P. (2008). Influence of morphology and permafrost dynamics on hyporheic exchange in arctic headwater streams under warming climate conditions. *Geophysical Research Letters*, *35*(2). https://doi.org/10.1029/2007GL032049

Zarnetske, J. P., Haggerty, R., Wondzell, S. M., & Baker, M. A. (2011a). Dynamics of nitrate production and removal as a function of residence time in the hyporheic zone. *Journal of Geophysical Research*, *116*(G1), G01025. https://doi.org/10.1029/2010JG001356

Zarnetske, J. P., Haggerty, R., Wondzell, S. M., & Baker, M. A. (2011b). Labile dissolved organic carbon supply limits hyporheic denitrification. *Journal of Geophysical Research*, *116*(G4), G04036. https://doi.org/10.1029/2011JG001730

Zarnetske, J. P., Haggerty, R., Wondzell, S. M., Bokil, V. A., & González-Pinzón, R. (2012). Coupled transport and reaction kinetics control the nitrate source-sink function of hyporheic zones. *Water Resources Research*, *48*(11). https://doi.org/10.1029/2012WR011894

Zhou, C., Liu, Y., Liu, C., Liu, Y., & Tfaily, M. M. (2019). Compositional changes of dissolved organic carbon during its dynamic desorption from hyporheic zone sediments. *Science of the Total Environment*, *658*, 16–23. https://doi.org/10.1016/j.scitotenv.2018.12.189